the benzamil-sensitive conductance was calculated from reversal potential $(E_{\rm rev})$ measurements using the Goldman-Hodgkin-Katz equation $[E_{\rm rev}=RT/zF]$ ln $(P_{\rm Na}[{\rm Na}])/(P_{\rm K}[{\rm K}])$.

Statistics

All values are presented as means \pm SEM, n is the number of monolayers, and N the number of animals in each experiment. The differences between control and treatment means were analyzed using a t-test for paired or unpaired means where appropriate. A value of P < 0.05 was considered statistically significant. IC₅₀ values were determined using a four-parameter logistic function to fit the data (PrismTM 2.0, GraphPad Software, Inc., San Diego, CA). The concentration of each compound at 50% maximal effect was determined from the equation.

RESULTS Short-term effect of EGF on I_{sc}

Addition of 1.6 nM (10 ng/ml) EGF to the basolateral solution of cell monolayers produced a decrease in basal $I_{\rm sc}$ from $37\pm3\,\mu{\rm A}$ to $5\pm1\,\mu{\rm A}$ (n=13,N=5) as illustrated in Figure 1A. Subsequent addition of 850 nM insulin to the basolateral solution produced no additional change in $I_{\rm sc}$. In Figure 1B, addition of 850 nM insulin stimulated the $I_{\rm sc}$ by $37\pm3\,\mu{\rm A}$ (n=6,N=4). Subsequent addition of EGF inhibited both insulin-stimulated $I_{\rm sc}$ and basal $I_{\rm sc}$ from $67\pm5\,\mu{\rm A}$ to $3.5\pm0.5\,\mu{\rm A}$ (n=6,N=4). Similar to EGF, the insulin-stimulated $I_{\rm sc}$ and the basal $I_{\rm sc}$ were inhibited by addition of $1.5\,\mu{\rm M}$ ionomycin to both apical and basolateral solutions as presented in Figure 1C.

Long-term effect of EGF on basal and benzamil-sensitive I_{sc}

The effects of growth factors on basal $I_{\rm sc}$ and benzamilsensitive I_{sc} are shown in Figure 2. Cells were allowed to grow in standard media for 1 week and replaced with serum-free media alone or serum-free media supplemented with growth factors (either insulin, IGF-1, EGF or $TGF\alpha$) for 4 days. In standard media, 20% of the basal I_{∞} was inhibited by the Na channel blocker, benzamil (5 μ M). The average basal $I_{\rm sc}$ and benzamil-sensitive $I_{\rm sc}$ were $34 \pm 3 \,\mu\text{A}$ and $8 \pm 2 \,\mu\text{A}$ (n = 12, N = 5) respectively. The basal $I_{\rm sc}$ was markedly decreased in serum-free media (13 \pm 2 μA) with no change in benzamil-sensitive $I_{sc}(9\pm 2 \mu A, n=9, N=4)$. Addition of 850 nM insulin or 1.3 nM IGF-I to the basolateral bathing media significantly increased $I_{\rm sc}$ (48 \pm 3 μA for insulin and 27 \pm 5 μA for IGF-I) and also stimulated the benzamil-sensitive $I_{\rm sc}$ (41 ± 3 μ A, n=23, N=10 for insulin and 23 ± 5 μ A, n=7, N=5 for IGF-I). Under insulin or IGF-I treatment conditions, the benzamil-sensitive I_{sc} accounted for 82-85% of the basal $I_{\rm sc}$ (Fig. 2A). Addition of 1.6 nM EGF to the bathing media for 4 days also significantly increased the basal $I_{\rm sc}$ (45 ± 4 μ A), however, the benzamil-sensitive $I_{\rm sc}$ was reduced (1.7 ± 0.4 μ A, n = 6, N = 4) when compared to serum-free media conditions. The same results were obtained when the cells were treated with 2 nM TGF α with a basal I_{sc} of $53 \pm 3 \,\mu\text{A}$ and a benzamilsensitive I_{sc} of $7 \pm 1 \mu A$ (n = 5, N = 3). Under EGF and TGFa treatment, the benzamil-sensitive Isc accounted

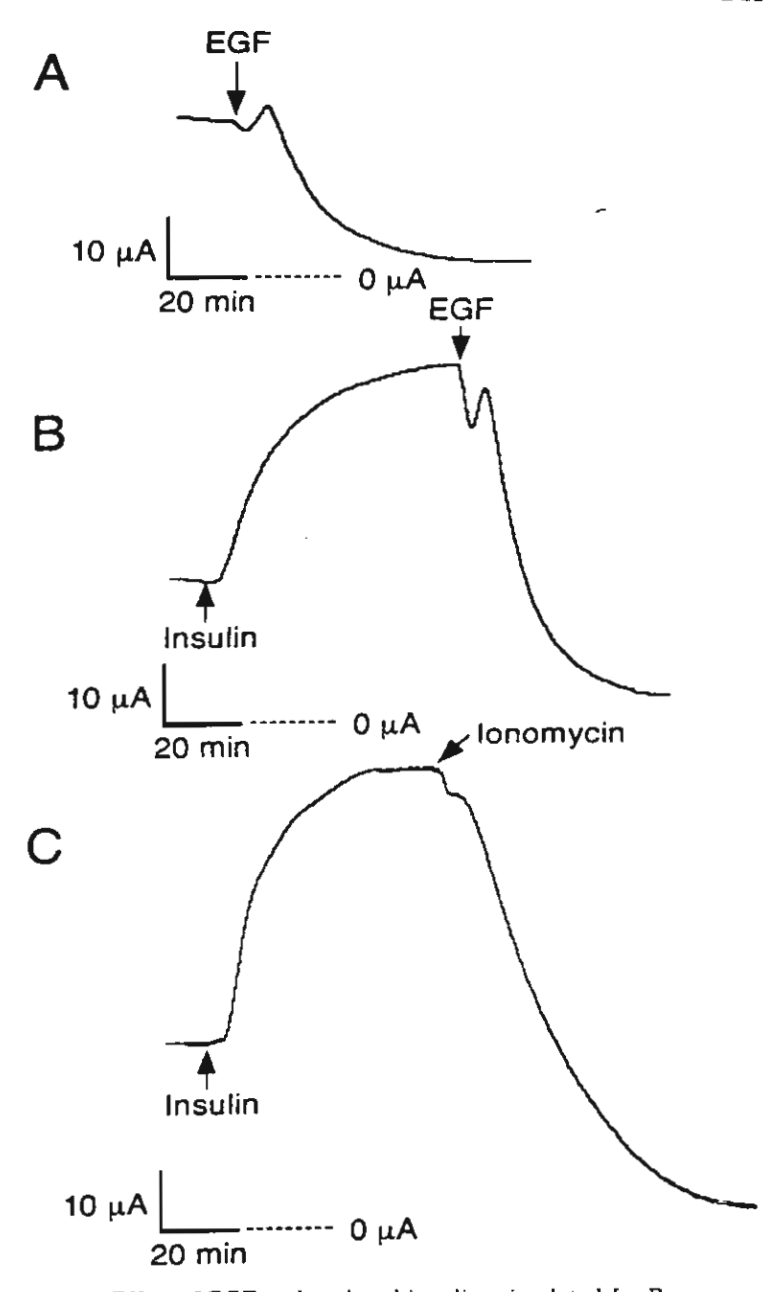
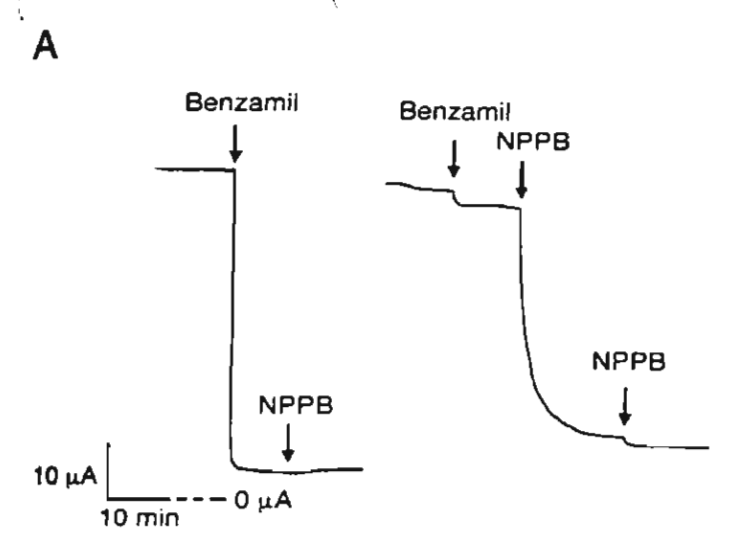


Fig. 1. Effect of EGF on basal and insulin-stimulated $I_{\rm sc}$. Representative tracings showing the decrease in $I_{\rm sc}$ following addition of 1.6 nM EGF to the basolateral solution of monolayers grown in serum-free media for 4 days. A: EGF produced a slow decrease in basal $I_{\rm sc}$ within 15 min and reached a minimum plateau in 1 h. B: EGF also decreased the $I_{\rm sc}$ stimulated by 850 nM insulin added to the basolateral solution. C: Addition of 1.5 μ M ionomycin to both apical and basolateral solutions produced a similar decrease in insulin-stimulated $I_{\rm sc}$.

for 4–14% of the basal $I_{\rm sc}$ and the remaining current was inhibited by the Cl⁻ channel blocker NPPB, as illustrated in Figure 2A.

Effect of EGF on ouabain-sensitive current across the basolateral membrane

In the following experiment we addressed the question of whether inhibition of insulin-stimulated Na absorption by EGF involved a direct inhibitory effect on Na-K-ATPase activity. Experiments were perfor-



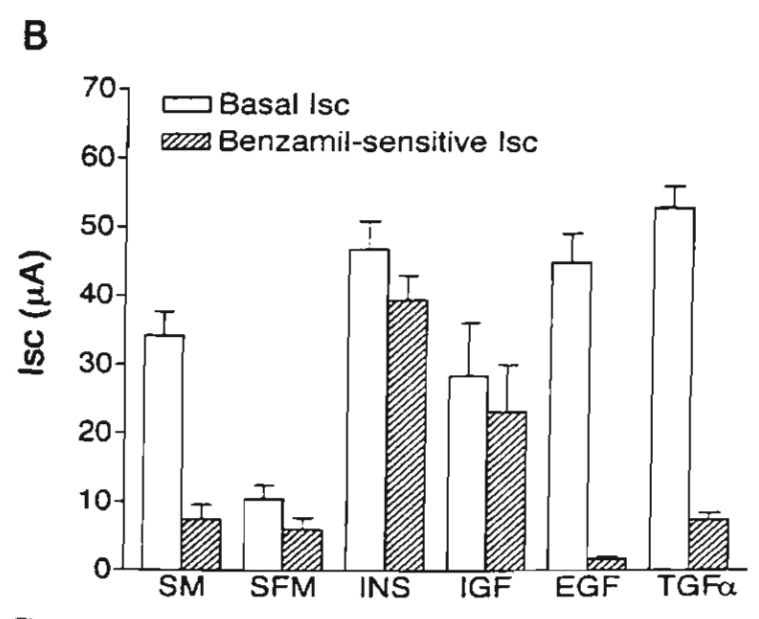


Fig. 2. Long-term effects of insulin, IGF-I, EGF and TGF α on basal and benzamil-sensitive I_{sc} . A: Representative tracings showing the decrease in I_{sc} after addition of 5 μ M benzamil to the apical solution of the cells grown in the presence of insulin (left panel) and EGF (right panel) for 4 days. The subsequent additions of 100 μ M NPPB to the apical solution produced a large decrease in the remaining I_{sc} of EGF-treated cells. B: Bar graph illustrating the basal I_{sc} and the absolute decrease in I_{sc} after addition of 5 μ M benzamil to the apical solution. Cells were treated with 850 nM insulin or 1.3 nM IGF-I, 1.6 nM EGF and 2 nM TGF α for 4 days (SM, serum-containing media; SFM, serum free media; INS, insulin; IGF, IGF1). Insulin, IGF-1, EGF and TGF α were added to cells maintained in serum free media.

med using amphotericin B-permeabilized (apical membrane) monolayers mounted in Ussing chambers. The apical surface of the epithelium was bathed with KMeSO₄ saline solution while standard saline solution was used to bathe the basolateral surface. The basolateral membrane voltage was held at 0 mV. Pump current was determined by subtracting the initial current before and 10 min after basolateral addition of 100 μM ouabain (Fig. 3). The ouabain-sensitive current after pretreat-

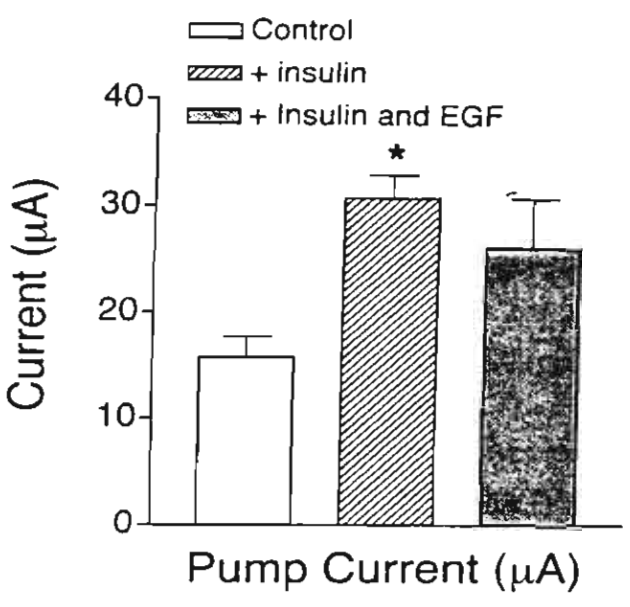


Fig. 3. Effects of EGF on ouabain-sensitive current in the basolateral membrane. Monolayers were bathed on the basolateral surface with standard Ringer solution and the apical surface with KMeSO₄ Ringer solution with 5 mM NaCl. Amphotericin B (10 μ M) was used to permeabilize the apical membrane. Ouabain (100 μ M) was added to the basolateral solution of the monolayers grown in serum-free media for 2 days. The ouabain-sensitive current is shown before (n=5, N=4) and after treatment with 850 nM insulin (n=6, N=4) added to the basolateral membrane. The following addition of 1.6 nM EGF after insulin treatment had no significant change in the ouabain-sensitive current (n=6, N=3)

ment with insulin for 15 min was approximately twofold greater in magnitude compared with the current measured under basal conditions. Addition of 1.6 nM EGF after insulin treatment had no significant effect on the ouabain-sensitive current, suggesting that EGF had no effect on insulin-dependent stimulation of the pump.

Effect of EGF on benzamil-sensitive, apical membrane Na conductance

Experiments were performed with amphotericin Bpermeabilized monolayers under conditions where the basolateral surface of the epithelium was permeabilized and bathed with KMeSO₄ saline solution and NaMeSO₄ saline solution was used to bathe the apical surface. Apical membrane voltage was held at 0 mV and then stepped from -100 to +160 mV in 10-mV increments. The current-voltage relationship for the benzamil-sensitive current obtained from cells treated with insulin (850 nM) for 4 days is shown in Figure 4. The benzamilsensitive current exhibited slight inward rectification with a mean reversal potential of 65 ± 4 mV (n = 7) and the Na:K selectivity ratio was calculated to be 11.6:1. Cells grown in the presence of insulin and EGF (1.6 nM) showed a significantly decreased Na + conductance from 0.37 ± 0.05 mS for insulin treatment (4 days) alone to 0.04 ± 0.02 mS and 0.07 ± 0.01 mS for 1 h and 4 days of treatment with EGF, respectively. No significant change in reversal potential was observed following treatment with EGF at either 1 h or 4 days.

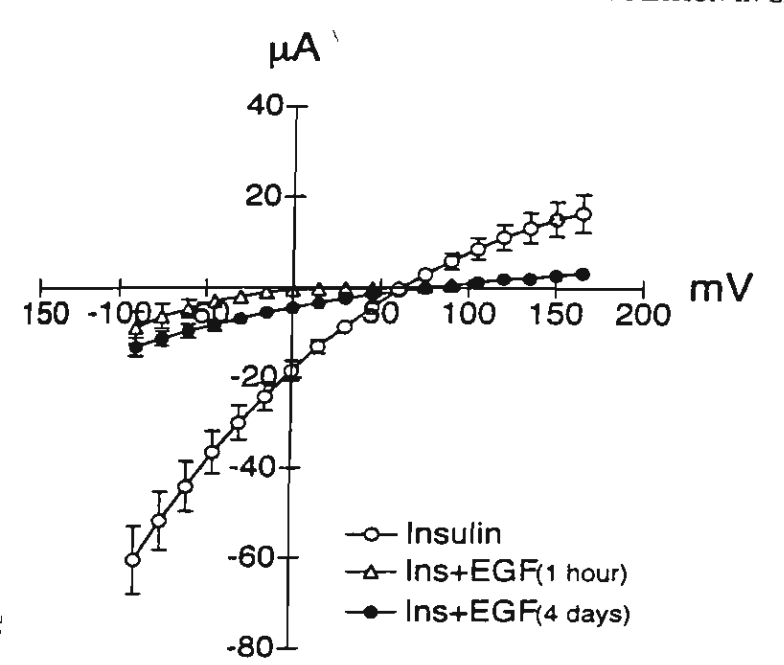


Fig. 4. Effects of EGF on apical benzamil-sensitive Na permeability. The benzamil-sensitive component of the apical membrane current is plotted as a function of voltage. Experiments were performed under conditions where the basolateral surface was bathed in KMeSO₄ saline solution with 5 mM NaCl and permeabilized with amphotericin B. NaMeSO₄ saline solution with 5 mM KCl was used to bathe the apical surface of the epithelium. Benzamil (5 μ M) was added to the apical solution of the cell monolayers treated with 850 nM insulin for 4 days (n = 7, N = 4) or with 850 nM insulin in the presence of 1.6 nM EGF for 4 days (n = 5, N = 3, long-term) or 1 h (n = 5, N = 3, shorterm). Mean reversal potentials for benzamil-sensitive currents were 65 \pm 4 mV, 68 \pm 1 mV and 55 \pm 5 mV for insulin alone, insulin \pm EGF for 1 h and insulin \pm EGF for 4 days, respectively.

Long-term effect of EGF on insulin-stimulated I_{sc}

The absolute decrease in $I_{\rm sc}$ in response to 5 μ M benzamil after 4 days of treatment with 850 nM insulin and EGF concentrations ranging from 0.016 to 16 nM is shown in Figure 5. EGF inhibited the insulin-stimulated, benzamil-sensitive $I_{\rm sc}$ with an estimated IC₅₀ value of 0.32 nM.

Effect of EGF on basal anion secretion

Cells treated with EGF for 4 days showed an increase in basal $I_{\rm sc}$, which was inhibited by NPPB, suggesting that EGF increased basal anion secretion (Fig. 6A). An initial increase in basal $I_{\rm sc}$ by EGF was observed on day 1 which averaged from $13\pm 2~\mu{\rm A}~(n=9,N=4)$ in serumfree media to $32\pm 5~\mu{\rm A}~(n=7,N=4)$ in EGF containing media. The increase in basal $I_{\rm sc}$ by EGF was abolished when cells were treated with 50 ng/ml actinomycin D ($12\pm 2~\mu{\rm A},~n=5,~N=3$) or 100 ng/ml cyclohexamide ($6.8\pm 0.7~\mu{\rm A},~n=11,~N=5$) for 1 day (Fig. 6A). The benzamil-sensitive $I_{\rm sc}$ decreased from $3.4\pm 0.8~\mu{\rm A}$ for EGF alone to $1.6\pm 0.6~\mu{\rm A}$ and $0.8\pm 0.5~\mu{\rm A}$ for EGF with actinomycin D and cyclohexamide, respectively. Figure 6B demonstrates that the absolute increase in $I_{\rm sc}$ after addition of 3 $\mu{\rm M}$ PGE2 to the basolateral solution of EGF, EGF + actinomycin D or EGF + cyclohexamide

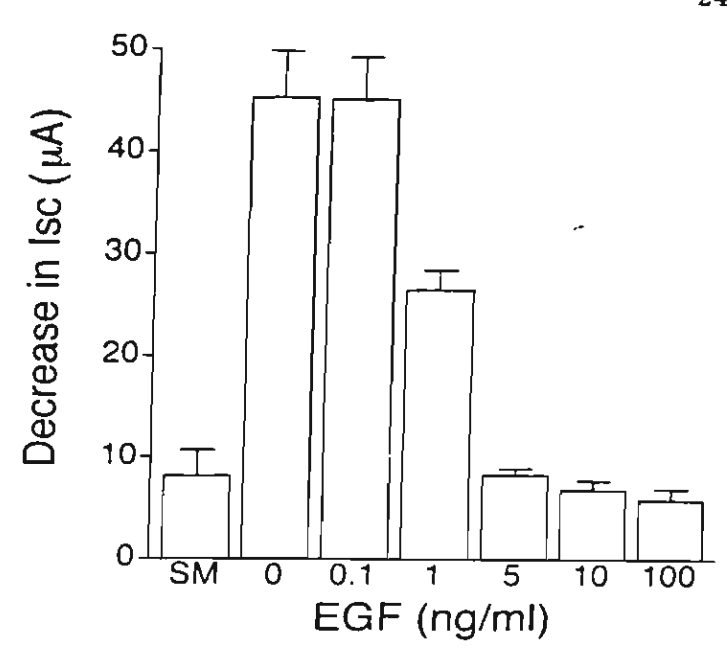


Fig. 5. Effect of EGF on insulin-stimulated $I_{\rm sc}$. Bar graph illustrating the absolute decrease in $I_{\rm sc}$ after addition of 5 $\mu{\rm M}$ benzamil to the apical solution of monolayers treated with 850 nM insulin in the presence of various concentrations of EGF for 4 days $(n={\rm at\ least\ 5}\ {\rm and\ } d)$ at least 3 in each experiment). Single concentrations of EGF were applied to groups of at least five monolayers at each concentration shown in the graph. The IC50 value for EGF-inhibited, insulinstimulated Na absorption was 0.3 nM.

treated monolayers were not significantly different with an average increase of $29\pm4~\mu A$ for EGF alone and $29\pm7~\mu A$ and $29\pm3~\mu A$ for EGF with actinomycin D and cyclohexamide, respectively. In addition, we also observed that treatment of monolayers maintained under serum-free conditions also responded in a similar manner to stimulation with 3 μM PGE $_2$ indicating that transport proteins required for anion secretion are present but not active in the absence of serum or EGF treatment.

Effects of EGF and TGFα on autocrine regulation of ion transport by prostaglandins

EGF has been shown to stimulate prostaglandin production in primary cultures of endometrial cells (Bany and Kennedy, 1995). Since PGE2 stimulates Cl⁻ secretion in endometrial epithelial cells (Deachapunya and O'Grady, 1998), we investigated whether a portion of the increase in anion secretion produced by EGF results from an increase in prostaglandin production and release from the epithelium. The absolute decrease in $I_{\rm sc}$ following addition of the cyclooxygenase inhibitor indomethacin (10 μ M) to both apical and basolateral solutions at the beginning of the experiment is shown in Figure 7. The indomethacin-sensitive $I_{\rm sc}$ significantly increased following EGF or TGFx-treatment.

DISCUSSION

Specific binding sites for EGF have been previously identified in glandular epithelial cells and stromal cells

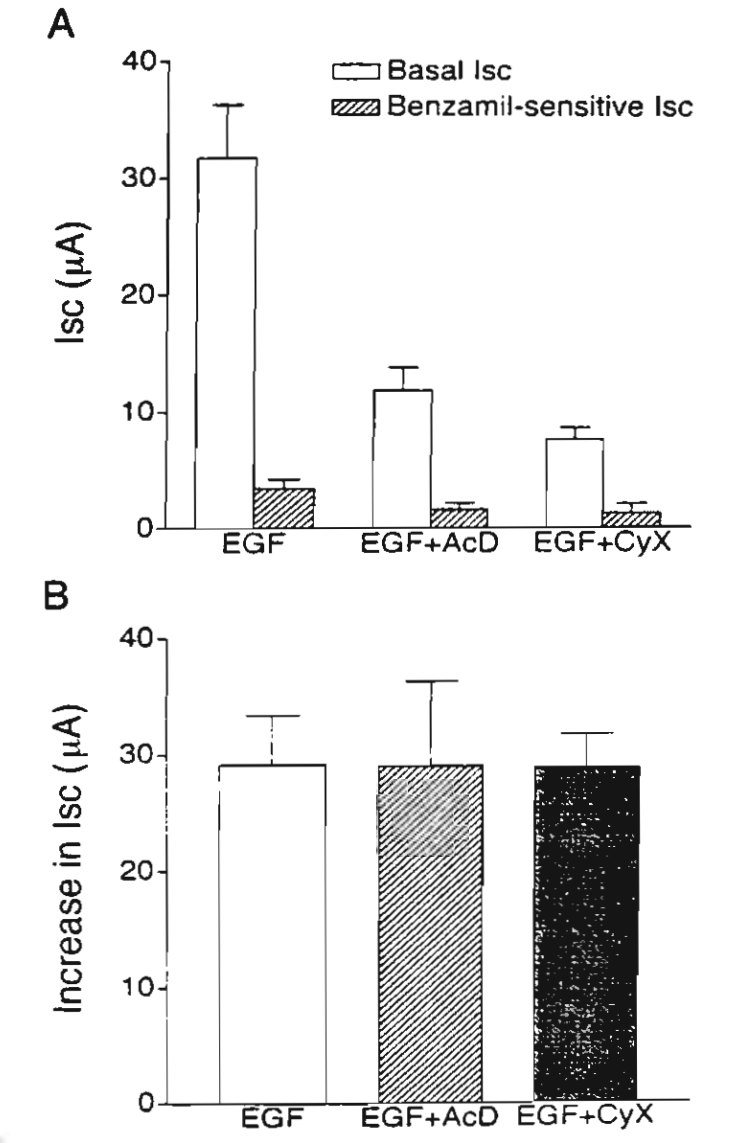


Fig. 6. Effects of actinomycin D and cycloheximide on EGF-stimulated anion secretion. (A) Bar graph illustrating the basal $I_{\rm sc}$ and the absolute decrease in $I_{\rm sc}$ after addition of 5 μ M benzamil to the apical solution of monolayers. (B) The absolute increase in $I_{\rm sc}$ after subsequent addition of 3 μ M PGE₂ to the basolateral solution of the same monolayers. The cells were treated with 1.6 nM EGF alone (n=7,N=4) or EGF with 50 ng/ml actinomycin D (AcD), (n=5,N=3) or 100 ng/ml cycloheximide (CyX) (n=11,N=5) for 24 h.

isolated from pig endometrium (Zhang et al., 1992). In the present study, EGF and TGF α inhibited Na⁺ absorption when added to the basolateral solution, but not the apical solution, suggesting that receptors for these growth factors were localized to the basolateral membrane. The ionic basis of the transient increase in I_{sc} shortly after EGF addition to the basolateral solution is not understood but could involve a transient stimulation of anion secretion as basal Na⁺ transport decreases. The EGF-dependent decrease in I_{sc} results from reducing Na⁺ entry through benzamil-sensitive Na channels located in the apical membrane. This conclusion is supported by the observation that the decrease in I_{sc} was temporally associated with a decrease in slope of

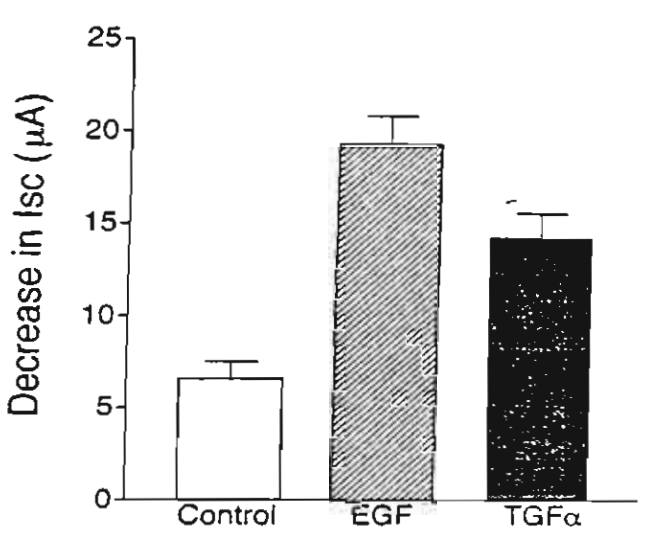


Fig. 7. Effects of EGF and $TGF\alpha$ on indomethacin-sensitive basal current. Bar graph illustrating the absolute decrease in I_{∞} after addition of 10 μ M indomethacin to both the apical and basolateral solution of monolayers treated with serum-free media (n=9, N=5), 1.6 nM EGF (n=17, N=6) or 2 nM $TGF\alpha$ (n=12, N=5) for 4 days.

the benzamil-sensitive current-voltage relationship. EGF was also found to inhibit insulin-stimulated Na absorption by reducing apical membrane Na - conductance, but had no effect on insulin-dependent stimulation of Na-K-ATPase activity. Moreover, pretreatment of monolayers with EGF was shown to block insulinstimulated increases in benzamil-sensitive Na absorption in a concentration-dependent manner with half maximum inhibition at 0.32 nM. This IC₅₀ value is in a range that was previously reported for the effects of EGF on prostaglandin production (Bany and Kennedy, 1995; Mitchell, 1991). In addition, the inhibitory actions of EGF on Na+ transport reported in this study are in agreement with those observed in cortical collecting duct where acute exposure to peritubular EGF inhibited the transepithelial Na - flux and produced significant hyperpolarization of the apical membrane, consistent with a reduction in Na + conductance (Vehaskari et al., 1991; Warden and Stokes, 1993).

Several growth hormones, including EGF, require an increase in cytosolic Ca2+, derived from intracellular stores to stimulate mitogenesis (Moolenaar et al., 1986; Chen et al., 1987). Mobilization of intracellular Ca²⁺ following stimulation of the EGF receptor has been shown in some cell types to be the result of EGF-receptor coupling to phospholipase C-y (PLC). At the present time, there is some evidence to indicate that the inhibitory effect of EGF on Na transport involves an increase in intracellular Ca²⁺ (Frindt and Windhager, 1990; Hebert et al., 1991; Vehaskari et al., 1991). In the present study, we found that increasing intracellular $[Ca^{2+}]$ with ionomycin could mimic the effect of EGF on I_{sc} , suggesting some role for Ca^{2+} or PKC in EGF signaling. Another possible mediator of EGF action on Na transport could be arachidonic acid since EGF is known to stimulate arachidonic acid synthesis (Nakano et al., 1995) and experiments with A6 epithelial cells have shown that apical release of arachidonic acid inhibits

epithelial Na channels (Worrell et al., 1999). Indirect evidence for EGF stimulation of arachidonic acid synthesis and metabolism was observed in the present study as indicated by a two- to three- fold increase in indomethacin sensitive I_{sc} reported in Figure 7 following **EGF** or $TGF\alpha$ stimulation.

In contrast to the acute inhibitory effects of EGF on Na transport in cortical collecting duct and in endometrial epithelial cells, long-term (12 h) exposure of alveolar epithelial cells to EGF produced an increase in amiloride-sensitive Na absorption (Borok et al., 1996). In the present study, we observed that exposure to EGF for a period of 24 h produced an increase in I_{sc} that was blocked by inhibitors of Cl channel activity in the apical membrane. Our results indicated that long-term treatment with EGF stimulated basal Cl secretion, similar in magnitude to that which was previously observed when endometrial epithelial cells were cultured in the presence of serum. Moreover, increases in Cl secretion produced by EGF or TGF α were blocked by inhibitors of DNA transcription and protein synthesis. PGE $_2$ -stimulated Cl secretion was not affected by actinomycin D or cyclohexamide. Thus it appears that endometrial epithelial cells express the necessary Cl- transport proteins required to produce and sustain Cl secretion following PGE2 stimulation under serum free conditions and in the absence of EGF. We suggest that upregulation of basal Cl - secretion after several hours of exposure to EGF or TGF 2 may involve transcription and expression of a new population of Cl channels or the expression of regulatory proteins that control the basal activities of Cl transport proteins already present in the epithelium. Increased expression of specific protein inases or inhibition of phosphatases could be a result of long-term EGF stimulation that would alter phosphorylation states of anion transport proteins and perhaps enhance the basal Cl secretory activity of the mono-

In endometrium, EGF was previously shown to play an important role in uterine cell growth and differentiation, blastocyst implantation and prostaglandin production. EGF and TGF2 were shown to stimulate PGE2 and PGF₂₇ secretion by glandular epithelial and stromal cells isolated from pig and human uterus (Mitchell, 1991; Zhang et al., 1992). Studies in rat endometrium demonstrated that EGF increased prostaglandin production through a mechanism that involved an increase in cyclooxygenase activity (Bany and Kennedy, 1995). These observations suggest the possibility that EGF might act to increase prostaglandin release and in turn stimulate Cl secretion. By using indomethacin to inhibit cyclooxygenase activity, we demonstrated that treatment with EGF and TGF2 for 4 days significantly increased the indomethacin-sensitive I_{sc} that accounted for 35-40% of the basal I_{∞} . This result suggested that, in addition to its direct effect on basal Cl secretion, long-term treatment with EGF appears to stimulate Cl secretion presumably by increasing arachidonic acid metabolism, resulting in an increase in prostaglandindependent stimulation of Cl secretion. A similar finding was reported in col-29 cells where EGF-stimulated anion secretion was predominantly inhibited by the cyclooxygenase inhibitor, piroxicam (Chinery and Cox, 1995). It is worth noting however that prostaglandin

synthesis and release was not directly measured in the present study, thus additional experiments documenting the effects of EGF on prostaglandin synthesis will be needed to confirm the our results with indomethacin.

In conclusion, EGF and TGF are capable of producing significant changes in the basal transport properties of primary endometrial epithelial cells. Both growth factors acutely abolished Na transport by inhibiting benzamil-sensitive Na channels under basal and insulin-stimulated conditions. This effect may be due to release of arachidonic acid and subsequent inhibition of Na + channel activity, or could involve changes in intracellular [Ca2+] or PKC activity that, in turn, inhibit basal and insulin-stimulated Na+ transport across the epithelium. Long-term treatment with EGF increased basal Cl secretion and this effect was prevented by actinomycin D and cyclohexamide. This result suggested that long-term regulation of Cl secretion by EGF required DNA transcription and protein synthesis. EGF was also found to stimulate prostaglandin synthesis and release, which in turn produced autocrine stimulation of Cl - secretion across the monolayer. These observations indicate that EGF and TGF2 may play an important role in regulating the basal transport phenotype of the endometrial epithelium during phases of the reproductive cycle where local EGF or TGF a production is enhanced by circulating hormones such as estrogen.

ACKNOWLEDGMENTS

The authors wish to thank Melissa Palmer-Densmore for her help with some of the experiments and for her comments on the manuscript. This work was supported in part by a post-doctoral grant to Chatsri Deachapunya.

LITERATURE CITED

Bany BM, Kennedy TG. 1995 Regulation by epidermal growth factor of prostagiandin production and cyclooxygenase activity in sensitized rat endometrial stromal cells in vitro. J Reprod Fert 104:57-62.

Berchuck A, Soisson AP, Olt GL, Soper JT, Clarke-Pearson DL, Bast RC, McCarty KS, 1989. Epidermal growth factor receptor expression in normal and malignant endometrium. Am J Obstet Gynecol 161:1247-1252.

Borok Z, Hami A, Danto SI, Lubman RL, Kim K, Crandall ED. 1996. Effects of EGF on alveolar epithelial functional permeability and

active sodium transport. Am J Physiol 270:L559-L565. Chen WS, Lazar CS, Poenie M, Tsien RY, Gill GN. Rosenfeld MG. 1987 Requirement for intrinsic protein tyrosine kinase in the immediate and late actions of the EGF receptor. Nature 328:820-

Chinery R, Cox HM. 1995 Modulation of epidermal growth factor effects on epithelial ion transport by intestinal trefoil factor. Br J Pharmacol 115:77-80.

Davis DL, RM Blair. 1993. Studies of uterine secretions and products of primary cultures of endometrial cells in pigs. J Reprod Fert Supp 48:143-155

Danto SI, Borok Z, Zhang X-L, Lopez MZ, Patel P, Crandall ED, Lubman RL. 1998. Mechanisms of EGF-induced stimulation of sodium reabsorption by alveolar epithelial cells. Am J Physiol 275:C82-C92.

Deachapunya C, O'Grady SM. 1998. Regulation of chloride secretion across porcine endometrial epithelial cells by prostaglandin E2. J Physiol 508:31-47

Deachapunya C, Palmer-Densmore M, O'Grady SM, 1999, Insulin stimulates transepithelial sodium transport by activation of a protein phosphatase that increases Na-K ATPase activity in endometrial epithelial cells. J Gen Physiol 114:561-574.

Frindt G, Windhager EE. 1990. Ca² dependent inhibition of sodium

transport in rabbit cortical collecting tubules. Am J Physiol 258:

F568-F582.

Haining REB, Cameron IT, Van Papendorp C, Davenport AP, Prentice A, Thomas EJ, Smith SK. 1991. Epidermal growth factor in human endometrium: proliferative effects in culture and immunocytochemical localization in normal and endometriotic tissues. Hum Reprod 6.1200 - 1205

Hebert RL, Jacobson HR, Breyer MD. 1991. Prostaglandin E2 inhibits sodium transport in the rabbit CCD by raising intracellular calcium.

J Clin Invest 87:1992-1998.

Horvath K, Hill ID, Devarajan P, Mehta D, Thomas SC, Lu RB, Lebenthal E. 1994. Short-term effect of epidermal growth factor (EGF) on sodium and glucose cotransport of isolated jejunal epithelial cells. Biochim Biphys Acta 1222:215-222.

Kennedy TG, Brown KD, Vaughan TJ. 1994. Expression of the genes for the epidermal growth factor receptor and its ligands in porcine

oviduct and endometrium. Biol Reprod 50:751-756

Khurana S, Nath SK, Levine SA, Bowser JM, Tse C-M, Cohen ME, Donowitz M. 1996. Brush Border Phosphatidylinositol 3-kinase mediates epidermal growth factor stimulation of intestinal NaCl absorption and Na +/H - exchange. J Biol Chem 271:9919-9927

LeRoith D, Adamo M, Werner H, Roberts CT Jr. 1991. Insulin-like growth factors and their receptors as growth regulators in normal physiology and pathologic states. Trends Endocrinol Metals 2:134-139

Lingham RB, Stancel GM, Loose-Mitchell DS. 1988. Estrogen regulation of epidermal growth factor receptor messenger ribonucleic acid. Mol Endocrinol 2:230-235.

Mitchell MD. 1991. The regulation of decidual prostaglandin biosynthesis by growth factors, phorbol esters and calcium. Biol Reprod 44:871-874.

Moolenaar WH, Aerts RJ, Tertoolen LGJ, De Laat SW. 1986. The epidermal growth factor-induced calcium signal in A431 cells. J Biol Chem 261:279-284.

Nakano O, Sakamoto C, Matsuda K, Konda Y, Matozaki T, Nishisaki H, Wada K, Suzuki T, Uchida M. 1995. Induction of cyclooxygenase protein and stimulation of prostaglandin E2 release by epidermal growth factor in cultured guinea pig gastric mucous cells. Dig Dis Sci 40(8):1679–1686

Rozengurt E, Heppel LA. 1975. Serum rapidly stimulates ouabain-sensitive ⁸⁶Rb + influx in quiescent 3T3 cells. Proc Natl Acad Sci Heppel LA. 1975. Serum rapidly stimulates ouabain-

USA 72:4492-4495.

Uribe JM, Gelbmann CM, Traynor-Kaplan AE, Barrett KE. 1996. Epidermal growth factor inhibits Ca²⁺-dependent Cl transport in Epidermal growth factor inhibits Ca² dependent Cl transport in T₈₄ human colonic epithelial cells. Am J Physiol 271:C914-922.

Vehaskari VM, Herhdon J, Lee Hamm L. 1991, Mechanism of sodium transport inhibition by epidermal growth factor in cortical collecting

ducts. Am J Physiol 261:F896-F903.

Vetter AE, O'Grady SM. 1996. Mechanisms of electrolyte transport across the endometrium I. Regulation by PGF22 and cAMP. Am J Physiol 270:663-672

Warden DH, Stokes JB. 1993. EGF and PGE2 inhibit rabbit CCD Na ' transport by different mechanisms: PGE2 inhibits Na '-K' pump. Am J Physiol 264:F670-F677

Worrell RT, Bao H-F, Eaton DC. 1999. Apical and basolateral cPLA2 activity differentially modulates epithelial Na transport. FASEB J 13(4):A68.

Zhang Z, Krause M, Davis DL. 1992. Epidermal growth factor receptors in porcine endometrium: binding characteristics and the regulation of prostaglandin E and F22 production. Biol reprod 46:

UTP-dependent Inhibition of Na⁺ Absorption Requires Activation of PKC in Endometrial Epithelial Cells

Melissa Palmer-Densmore¹, Chatsri Deachapunya², Mathur Kannan³ and Scott M. O'Grady¹

From the ¹Departments of Physiology and Animal Science and the ³Department of Veterinary Pathobiology, University of Minnesota, St. Paul, Minnesota 55108, and the ²Department of Physiology, Faculty of Medicine, Srinakharinwirot University, Sukhumvit, Wattana, Bangkok, Thailand

Running Title: UTP inhibition of endometrial Na absorption

Address correspondence to: Dr. Scott M. O'Grady, Ph.D., Departments of Physiology and Animal Science, 495 Animal Science/Veterinary Medicine Building,

University of Minnesota, St. Paul, MN 55108.

Telephone: (612) 624-3767;

Fax: (612) 625-2743;

E-mail address: ograd001@umn.edu

ABSTRACT

The objective of this study was to investigate the mechanism of UTP-dependent inhibition of Na $^+$ absorption in porcine endometrial epithelial cells. Acute stimulation with UTP (5 μ M) produced inhibition of sodium absorption and stimulation of chloride secretion. Experiments using basolateral membrane permeabilized cell monolayers demonstrated a reduction in benzamil-sensitive Na $^+$ conductance in the apical membrane following UTP stimulation. The UTP-dependent inhibition of sodium transport could be mimicked by PMA (1 μ M). Three different PKC inhibitors, Gö6983 (a nonselective inhibitor), rottlerin (a PKC8 selective inhibitor), and Gö6976 (a PKC α selective inhibitor), were shown to prevent UTP-dependent inhibition of the benzamil-sensitive Isc. In addition, treatment with a second nonselective PKC inhibitor, GF109203X, completely blocked the reduction in benzamil-sensitive Na $^+$ conductance following UTP stimulation. Finally, inhibition of the benzamil-sensitive Isc by UTP was observed in the presence of BAPTA-AM (50 μ M), confirming that activation of PKC, and not increases in [Ca $^{2+}$], alone, were directly responsible for the inhibition of apical Na $^+$ channels and transepithelial Na $^+$ absorption.

Keywords: P2Y receptor, ENaC, benzamil, chloride secretion, calcium-activated chloride channel

INTRODUCTION

In porcine endometrium, surface epithelial cells exhibited a basal Na⁺ absorption that was inhibited by amiloride and regulated by PGF2a⁺ and cAMP (Vetter and O'Grady, 1996). More recent studies using glandular endometrial epithelial cells in culture showed distinct basal transport phenotypes depending on the growth factor used to maintain the cells (Deachapunya and O'Grady, 2001; Deachapunya et al., 1999). Basal benzamil-sensitive sodium absorption was characteristic of glandular endometrial cell monolayers grown under serum-free conditions, or in the presence of insulin or insulin-like growth factor (IGF-1). Acute stimulation with insulin or IGF-1 enhanced sodium absorption by increasing Na⁺-K⁺ ATPase transport activity and basolateral membrane K⁺ conductance, without increasing the apical membrane benzamilsensitive Na⁺ conductance. The enhanced Na⁺-K⁺ ATPase activity was due to activation of phosphatidylinositol 3-kinase and subsequent stimulation of a protein phosphatase. Long-term

treatment with insulin additionally enhanced sodium absorption with a further increase in Na⁺-K⁺ ATPase activity and benzamil-sensitive Na⁺ conductance.

P2Y receptors have been identified on the apical membrane of both mouse and porcine endometrial cells (Chan et al, 1997; Palmer-Densmore et al, 2000). Most P2Y receptor subtypes are G-protein receptors that couple to Gq and activate phospholipase C (PLC) upon agonist stimulation. PLC activation subsequently initiates both diacylglycerol (DAG) and inositol 1,4,5trisphosphate (IP3) production, resulting in activation of protein kinase C (PKC) and increases in intracellular calcium concentrations ([Ca²⁺]_i). Previous studies have shown that ATP or UTPdependent increases in [Ca2+]; stimulate chloride secretion in both porcine and mouse endometrial epithelial cells (Palmer-Densmore et al, "chapter in book submitted"; Chan et al. 2000). In these cells, a DIDS-sensitive, Ca²⁺-activated anion channel has been identified in the apical membrane and is an essential component of Ca2+-dependent anion secretion. basolateral membrane permeabilized porcine endometrium, ion replacement experiments show that the UTP-activated current is both chloride and bicarbonate-dependent. activating apical Cl channels, UTP opens basolateral K channels. Two of these K channels have been identified in porcine endometrial epithelial cells and are activated by increases in either [Ca²⁻]; or PKC, thus providing the driving force for sustained chloride efflux across the apical membrane.

P2Y receptor activation has been found to decrease sodium absorption in mouse endometrial epithelial cells (Wang and Chan. 2000). In addition, UTP was found to inhibit sodium absorption in wild type and mutant CFTR-expressing human bronchial epithelia, as well as nasal epithelia from normal and cystic fibrosis patients (Devor and Pilewski, 1999; Mall et al, 2000). However, the mechanism for UTP-dependent inhibition of sodium absorption is not well understood. In the present study, we investigated the effects of UTP on the Na⁺ transport properties of primary endometrial epithelial cells grown in the absence of serum or presence of insulin. UTP was found to produce a dramatic inhibition of Na⁺ transport that involved a decrease in apical membrane Na⁺ conductance. We demonstrated that inhibition of benzamilsensitive Na⁺ channels was dependent on PKC activation and was not directly dependent on increases in [Ca²⁺]_i.

MATERIALS AND METHODS

Materials

UTP, 1,2-bis (2-aminophenoxy) ethane–N, N, N', N'-tetraacetic acid tetrakis (acetoxymethyl ester) (BAPTA-AM), insulin, indomethacin, non-essential amino acid and high purity grade salts were purchased from Sigma Chemical (St. Louis, MO). 5-nitro-2-(3-phenylpropylamino) benzoic acid (NPPB) was purchased from Research Biochemical International (Natick, MA) and benzamil from Molecular Probes (Eugene, OR). Gö6983, Gö6976 and rottlerin were obtained from Biomol (Plymouth Meeting, PA). Dulbecco's modified Eagle's medium (DMEM), Dulbecco's phosphate buffer saline (DPBS), fetal bovine serum (FBS), collagenase type 1, kanamycin, penicillin-streptomycin and fungizone were purchased from Gibco BRL (Grand Island, NY).

Cell isolation and culture

The epithelial glands were isolated from pig uterus as described previously (Deachapunya and O'Grady, 1998). The isolated glands were suspended in DMEM supplemented with 3.7 g/L sodium bicarbonate, 10% FBS, 5 μg/ml insulin, 1% non-essential amino acid, 5 μg ml fungizone, 100 U/ml penicillin, 100 μg/ml streptomycin and 100 μg/ml kanamycin (standard media). They were plated onto cell culture dishes and incubated at 37°C in a humidified atmosphere of 5% CO₂ in air. Culture medium was changed after 24 hours and then every 2-3 days. After 80% confluency (within 2-3 days), the stromal cells were easily removed by trypsinization for 5 minutes and the epithelial cells were further trypsinized and subcultured onto 24 mm (4.5 cm²) transparent permeable membrane filters (CoStar, Cambridge, MA). After plating on filters, monolayers were fed every two days and maintained in standard media for 7 days. The standard media was subsequently replaced with DMEM (serum-free media) or DMEM supplemented with 850 nM insulin for 3 days.

Measurement of monolayer electrical properties

Transepithelial resistance of the cell monolayers was measured using the EVOM epithelial voltohmmeter coupled to Ag/AgCl "chopstick" electrodes (World Precision Instruments, New Haven, CT). High resistance monolayers (~3000 Ω cm²) were mounted in Ussing Chambers, bathed on both sides with standard porcine saline solution containing (in

mM): 130 NaCl, 6 KCl, 1.5 CaCl₂, 1 MgCl₂, 20 NaHCO₃, 0.3 Na H₂PO₄, 1.3 Na₂HPO₄, pH 7.4, which was maintained at 37°C and bubbled with 95% O₂ / 5% CO₂. Transepithelial potential difference, monolayer conductance and short circuit current (Isc) were measured with the use of voltage-clamp circuitry from JWT Engineering (Overland Park, KS). The data from the voltage clamp experiments was digitized, stored and analyzed using Workbench data acquisition software (Kent Scientific Corporation, Litchfield, CT) and recorded with a Pentium microcomputer. All cells were pretreated with indomethacin (10 μM) added to both apical and basolateral solutions at least 10 minutes before the beginning of the experiment to eliminate endogenous prostaglandin production. PGE₂ is endogenously produced by porcine endometrial epithelial cells and has been shown to regulate Cl secretion (Deachapunya and O'Grady, 1998).

For experiments involving measurement of membrane conductance, amphotericin B (10 μM) was used to permeabilize the apical or basolateral membranes of the monolayers mounted in Ussing chambers. The permeabilized membranes were bathed with KMeSO₄ saline solution containing (in mM): 120 KMeSO₄, 5 NaCl, 3 calcium gluconate, 1 MgSO₄, 20 KHCO₃, 0.3 KH₂PO₄, 1.3 K₂HPO₄, 30 mannitol, pH 7.4, while the intact membranes were bathed with standard porcine saline solution. A World Precision Instrument epithelial voltage clamp (Sarasota, FL) was used to voltage clamp the monolayers. The data was recorded using a Pentium microcomputer with an Axon Instruments TL-1 interface. Voltage step commands and the resultant currents were generated and recorded using pCLAMP software (Axon Instruments). Current-voltage relationships were obtained by a series of voltage step commands described in the figure legends. The compound-sensitive current components were obtained by subtracting currents before and after addition of UTP or blocker compounds.

Measurement of intracellular calcium

Cells were seeded at low density on glass coverslips for 48 hours. After adhesion to the coverslips, the cells were washed with Hanks balanced salt solution (HBSS) containing 10 mM glucose, 10 mM HEPES, pH 7.4. The cells were then loaded with 10 µM fura-2-AM (Molecular Probes, Eugene, OR) for 45 minutes at 37°C, washed in HBSS, mounted onto a Plexiglas chamber (150 µl volume, Warner Instruments, Hamden, CT), and transferred to the stage of a Nikon Diaphot inverted microscope with an epifluorescence attachment. The chamber was perfused with HBSS at 2-3 ml / minute at room temperature. Fluorescence in single cells was

visualized using a Nikon UV-fluor 40X oil-immersion objective. The fluorescence excitation, image acquisition and real-time data analyses were controlled by the Image-1 Metamorph software (Universal Imaging, Westchester, PA) running on a Pentium microcomputer. $[Ca^{2+}]_1$ was measured as the ratio of fluorescence emitted at 510 nm when the cells are alternately excited at 340 nm and 380 nm $[F_{340}/F_{380}]$.

Western Blot Analysis

Cell monolayers were solubilized with lysis buffer (50mM Tris-HCl, 1% NP-40, 0.25% sodium deoxycholate, 150mM NaCl, 1mM EGTA, 1mM PMSF, 1 µg/ml aprotinin, and 1mM NaF, pH 7.4) at 37°C for 30 minutes. A protein assay was performed using a BCA Protein Assay Kit by Pierce. Proteins were separated by PAGE (8%). Electroblotting was done using Immobilon-P (Millipore Corp.). The electroblot assembly was placed into the electroblotting apparatus (Trans-Blot Cell; Bio-Rad Laboratories) and blotting was performed at 16V overnight on ice. After the blots were removed, they were washed twice, and then blocked in freshly prepared 1X TBS-tween containing 3% nonfat dry milk (MLK) for 1 hour at 20-25°C with constant agitation. After washing, blots were reacted overnight in primary antibody. 15 ml freshly prepared 1X TBS-tween containing 3% MLK with appropriate dilution of the primary antibody (human anti-rabbit PKC α , $\beta 1_1$, $\beta 2_1 \delta$, ζ , ϵ , θ , μ , η polyclonal antibody from Santa Cruz Biotechnology). The next day, blots were washed and reacted with secondary antibody, alkaline phosphatase-labeled goat anti-rabbit. Secondary antibody was diluted 1:3000 in 1X TBS-tween containing 3% MLK and was reacted for 1-2 hour. After washing, alkaline phophatase color reagent was added to 100 ml 1X alkaline phosphatase color development buffer at room temperature. Blots were incubated in development buffer until bands were clearly developed.

Statistics

All values are presented as means \pm S.E.M., n is the number of monolayers and N is the number of animals in each experiment. The differences between control and treatment means were analyzed using a t-test for paired and unpaired means where appropriate. A value of P<0.05 was considered statistically significant.

RESULTS

Acute effects of UTP on sodium absorption and chloride secretion. The basal electrical properties of cultured porcine endometrial epithelial cells have been previously described (Deachapunya and O'Grady 2001, Deachapunya et. al. 1999 and Deachapunya and O'Grady 1998). In order to maximize basal sodium absorption, cells were cultured under serum-free conditions in the presence of insulin for three days. To determine the acute effects of UTP on basal sodium absorption and chloride secretion, cell monolayers were mounted in Ussing chambers and bathed on both sides with standard porcine saline solution. In Figure 1A, the basal short circuit current (Isc) was predominantly benzamil-sensitive, and the Cl- channel inhibitor, NPPB, blocked the remaining Isc. After the addition of UTP (5 μM), the new steady-state Isc was predominantly NPPB-sensitive (Fig. 1B), whereas the benzamil-sensitive Isc was nearly abolished after stimulation with UTP.

PMA mimics the effects of UTP on inhibition of sodium absorption. In order to illustrate further the inhibition of sodium absorption by UTP, cells were maintained under serum-free conditions and acutely stimulated with insulin (850 nM). Previous studies have characterized the acute insulin response as an increase in benzamil-sensitive sodium absorption resulting from enhanced Na⁻-K⁻-ATPase activity and an increase in basolateral membrane K⁻ conductance (Deachapunya and O'Grady, 1999). As shown in Figure 2A, addition of UTP (1 μ M) inhibited the insulinstimulated Isc and part of the basal Isc. This effect was mimicked by 1 μ M phorbol 12-myristate 13-acetate (PMA), an activator of protein kinase C (PKC), (Fig. 2B). To determine whether increases in intracellular calcium were responsible for PMA-mediated inhibition of sodium absorption, calcium-imaging experiments with fura 2 loaded primary endometrial cells were conducted. Addition of PMA (1 μ M) failed to show a detectable increase in intracellular calcium, whereas a concentration-dependent increase in [Ca²⁺], was observed after stimulation with 1 and 5 μ M UTP, (Fig. 2C).

Effects of UTP on sodium transport across the apical membrane. To investigate the effects of UTP on apical membrane Na⁺ conductance, benzamil-sensitive difference currents were determined from basolateral membrane permeabilized monolayers. Apical membrane currents were elicited using a voltage step protocol from -100 to +95 mV in 15 mV increments at a

holding potential of 0 mV. Benzamil (5 μ M) was added to the apical solution in the absence (control) or presence of 5 μ M UTP. The representative traces in Figure 3A show the benzamil-sensitive difference current without UTP (upper trace) and in the presence of apical UTP (lower trace). Figure 3B represents the benzamil-sensitive current-voltage relationship before and after UTP (1 μ M), where a decrease in apical membrane conductance was apparent after comparing the UTP-stimulated I-V relationship to unstimulated controls. Mean reversal potentials for benzamil-sensitive currents were 66.1 \pm 4.2 mV (n=5, N=3) for control and 57.9 \pm 6.3 mV (n=6, N=3) after UTP, and were not significantly different.

Chloride-dependent effects of UTP. Cell monolayers were placed in Ussing chambers and bathed on both sides with either chloride-containing or chloride-free saline solutions. A reduction in peak UTP-activated current was evident when comparing monolayers bathed in chloride-free solution to control cell monolayers, (Fig. 4A). In addition, a large reduction in NPPB-sensitive current also occurred, whereas no change in the benzamil-sensitive current was detected. (Fig. 4B). The effect of UTP on apical chloride conductance is shown in Fig. 5. UTP (1 μM) produced a rapid rise and gradual fall in apical membrane current, (Fig. 5A). The peak UTP-activated current was outwardly rectifying and chloride-dependent, (Fig. 5B). The voltage protocol used to obtain the UTP-activated current-voltage relationship ranged from -90 to +90 mV in 15 mV increments from a holding potential of 0 mV. The mean reversal potential was -28.4 ± 1.3 mV (n=6, N=4).

PKC regulation of sodium absorption. To study the possible role of PKC in UTP regulation of sodium absorption, a variety of PKC inhibitors were used in an attempt to block UTP-dependent inhibition of the benzamil-sensitive current. Figure 6A and B illustrate preservation of the benzamil-sensitive current after pretreatment with three different PKC inhibitors. Gö6983, a non selective PKC inhibitor, and rottlerin, a selective inhibitor of PKCδ, abolished the effects of UTP on benzamil-sensitive Isc, (n=9 and 5, respectively, N=2). In contrast, 100 nM and 10 μM Gö6976, a selective PKCα inhibitor, partially blocked the effects of UTP on the benzamil-sensitive current, (n=6 and 4, respectively, N=2). PMA (0.5 μM) mimicked UTP inhibition of the benzamil-sensitive current as shown previously in Fig. 2, (n=4 and 14, respectively, N=3).

The effects of the PKC inhibitor, GF109203X (5 μ M) on UTP-dependent regulation of the apical Na $^+$ conductance is shown in Fig. 6C. These conductance values were calculated according to Ohm's law using benzamil-sensitive apical membrane currents at 0 mV in the absence or presence of UTP (5 μ M), or following pretreatment with both GF109203X and UTP. The benzamil-sensitive conductance following UTP was diminished compared to the unstimulated controls. Pretreatment with GF109203X abolished the effects of UTP on the benzamil-sensitive conductance. In Figure 7, identification of PKC isoforms in whole cell lysates of endometrial epithelial cells was accomplished by western blot analysis of monolayers maintained under serum free conditions for 3 days. A total of nine PKC isoform-specific antibodies were tested representing classical, novel and atypical PKC isoforms. The results show that the calcium-dependent alpha isoform and two calcium-independent isoforms (delta and zeta) are expressed in these cells (the θ isoform was not detected, data not shown).

BAPTA-AM does not effect UTP-dependent inhibition of sodium absorption. Calcium imaging experiments show that mobilization of intracellular calcium by UTP (5 μM) was dramatically reduced after pretreatment with BAPTA-AM (50 μM), (Fig. 8). Initially, BAPTA-AM reduced the basal level of intracellular calcium by 80 nM, and upon stimulation with UTP. [Ca²⁺], increased by only 20 nM. In contrast, [Ca²⁺], increased three-fold from 75 nM to 230 nM after UTP treatment in control monolayers that were not pretreated with BAPTA-AM. Isc results correspond with calcium imaging data showing that peak UTP-activated currents were reduced in the presence of BAPTA-AM. However, UTP-dependent inhibition of the benzamil-sensitive current was unaffected by treatment with BAPTA-AM, (Fig. 9).

DISCUSSION

CFTR has been previously shown to regulate cAMP-dependent gating of epithelial sodium channels, resulting in increased Na⁺ absorption observed in CF patients. More recently, UTP has been identified as a potentially useful therapeutic agent for patients with cystic fibrosis as a result of several studies demonstrating that UTP stimulates Cl' secretion and inhibits amiloride-sensitive Na⁺ absorption in normal and CF airway epithelia. Therapeutic procedures for CF currently use amiloride to inhibit the apical membrane sodium conductance in CF patients. An advantage for using UTP in place of amiloride is that UTP can simultaneously

stimulate Cl secretion and inhibit Na absorption across the airway epithelium, and thus provide a means for compensating for the defect in CFTR expression in CF airways.

Since Mason et al. first demonstrated regulation of ion transport by purinergic receptors in normal and cystic fibrosis airway epithelium, the effects of ATP and UTP on sodium absorption have been studied in a variety of epithelial cell systems. Two examples include mouse inner medullary collecting duct (mIMCD) by McCoy et al. (1999) and mouse endometrial epithelium by Wang and Chan (2000). In these studies, most of the basal Isc was amiloridesensitive (~90%), consistent with Na+ absorption. However, only modest reductions (~10%) in amiloride-sensitive current were observed after treatment with ATP (10-100 µM) or UTP (100 μM). These relatively small decreases in amiloride-sensitive Isc may reflect changes in driving force for Na influx and may not be due to direct effects on apical Na conductance. Greater effects of ATP (100 μM) on amiloride-sensitive Isc were shown in mouse cortical collecting duct by Thomas et al. (2001). The ATP-dependent reduction in basal Isc was approximately onethird of the total amiloride-sensitive current, indicating that ATP-dependent inhibition of sodium absorption was also incomplete. In contrast to the effects of UTP on Na transport in mouse collecting duct and endometrium, more complete inhibition (40 to 75%) of amiloride-sensitive Na absorption after UTP was shown in porcine thyroid epithelial cells and airway epithelia. In these studies, different hypotheses were proposed to account for inhibition of sodium absorption based on experiments where the actions of ATP or UTP on intracellular calcium or PKC activity were investigated. Direct inhibition of sodium absorption mediated by calcium following stimulation with ATP or UTP was proposed in CFTR-expressing human bronchial epithelia, nasal airway epithelium and distal bronchi. In contrast, inhibition of Na absorption in mouse CCD cells by UTP were not mediated by either [Ca²⁺]; or PKC activation. PKC regulation of sodium absorption was demonstrated by Koster et al., where ATP and UTP were shown to inhibit sodium absorption in rabbit connecting tubule and cortical collecting duct cells. It is worth noting that in all of the studies cited above, conclusions regarding the effects of UTP on Na absorption were based on measurements of Isc. The specific effects of ATP or UTP on Na channel function were not directly measured. Thus, it is possible that decreases in Isc produced by P2Y receptor activation may be a consequence of inhibiting pathways other than apical Na⁺ In the present study, the significant reduction (80%) in benzamil-sensitive Isc following UTP stimulation was blocked by PKC inhibitors. Additionally, effects of the PKC

activator, PMA, were identical to the inhibitory effects of UTP on sodium absorption. UTP-dependent inhibition of sodium absorption was also observed in the presence of BAPTA-AM (50 µM), demonstrating that increases in $[Ca^{2+}]_i$ were not responsible for inhibiting sodium absorption in this system. The fact that decreases in apical membrane Na⁺ conductance produced by UTP could be blocked following pretreatment with the PKC inhibitor, GF109203X, confirmed that the target of UTP action on transepithelial Na transport was apical membrane Na channels.

Several previous studies have demonstrated that activation of PKC inhibits apical Na* channels. PKC-mediated inhibition of Na* channels was shown in rabbit cortical collecting tubules and in an amphibian renal cell line (A6) after acute PGE₂ stimulation. In these studies, PGE₂ was shown to inhibit highly selective apical membrane Na* channels by increasing Ca²*-dependent PKC activity, resulting in a decrease in channel open probability. In the present study, inhibition of sodium absorption appeared to depend on activation of both Ca²*-dependent and Ca²*-independent isoforms of PKC. PKC regulation of epithelial Na* channel function has also been demonstrated by Awayda et al. (1996, 2000) using purified Na* channel proteins reconstituted in planar lipid bilayers and cloned ENaC subunits expressed in *Xenopus* oocytes. Activation of PKC by PMA and direct injection of purified PKC inhibited whole-cell currents in ENaC-expressing oocytes. In planar lipid bilayers, addition of PKC, diacyl-glycerol and Mg-ATP decreased ENaC open probability. More recent studies by Awayda further describe the activation of PKC by PMA and subsequent inhibition of ENaC activity in oocytes, which included nonspecific effects on membrane capacitance.

Previous studies by Ishikawa et al. showed a biphasic inhibition of whole-cell Na⁺ currents in ENaC-expressing MDCK cells when $[Ca^{2+}]$, was increased to 1 μ M. This biphasic effect was due to an initial inhibition of Na⁺ current within the first 5 minutes, followed by a secondary decrease in ENaC activity that occurred between 100 and 160 minutes after raising $[Ca^{2+}]_i$. Stockand et al. (2000) subsequently demonstrated that treatment of A6 cells with PMA decreased the expression levels of β and γ , but not α ENaC. The time constant for the decline in γ and β ENaC expression was approximately 4 and 14 hours, respectively, consistent with long-term inhibition of ENaC. Furthermore, direct evidence for PMA-dependent phosphorylation of the carboxyl termini of β and γ ENaC subunits, but not the α ENaC subunit, was shown in a stably

transfected MDCK cell line. Thus, PKC activation following UTP stimulation may produce long-term inhibition of Na^{\dagger} absorption by decreasing the expression of β and γ subunits.

Studies in airway epithelia suggest that increases in $[Ca^{2+}]_i$ are responsible for inhibition of Na^+ absorption. Previous studies have shown Ca^{2+} block of ENaC activity in planar lipid bilayers. It is worth noting that open probability and single-channel conductance of $\alpha ENaC$ remained stable when $[Ca^{2+}]$ was varied within a physiologically relevant range, (between 10 nM and 1 μ M.) However, raising the $[Ca^{2+}]$ beyond 2 μ M produced a dose-dependent decrease in single-channel open probability ($K_D \sim 20~\mu$ M), or single-channel conductance ($K_D \sim 6~\mu$ M) if monomeric actin was present. Studies by Devor and Pilewski, and Mall *et al.* (1999 and 2000, respectively) suggest a role for Ca^{2+} in inhibiting Na^+ absorption, but the effects of UTP on $[Ca^{2+}]_i$, was not reported. Thus, it remains unclear whether UTP-dependent increases in $[Ca^{2+}]_i$ were sufficient in magnitude to produce inhibition of ENaC activity. Calcium imaging experiments in the present study show $[Ca^{2+}]_i$ increases following UTP stimulation were well below the $[Ca^{2+}]_i$ required to influence $\alpha ENaC$ activity in planar lipid bilayers. This result is consistent with our conclusion that calcium is not directly responsible for Na^+ channel inhibition in porcine endometrial epithelial cells.

The inhibitory effects of UTP on transepithelial Na absorption have been shown to differ significantly in magnitude and mechanism of regulation in a variety of epithelial cells types. One explanation for these differences is that PKC isoforms expressed in a given epithelial cell type are variable, and that inhibition of sodium absorption by PKC is isoform specific. Alternatively, variability in α , β and γ ENaC subunit expression in different epithelial cell types may also account for the varying levels of UTP effects on sodium absorption. In the present study, UTP was shown to inhibit benzamil-sensitive sodium absorption by 80% in porcine endometrial epithelial cells. This effect was due to direct inhibition of apical membrane sodium channels and was dependent on activation of PKC. These results are consistent with previous studies of PKC inhibition of ENaC activity and completely account for the decrease in Na absorption observed in porcine endometrial cells. The endometrial epithelium therefore represents a useful mammalian model cell system for further studies of P2Y-receptor mediated regulation and PKC-dependent regulation of epithelial Na channel function.

FOOTNOTES

'Abbreviations used in this paper: ATP, adenosine 5'-triphosphate; cAMP, adenosine 3',5'-cyclic monophosphate; CF, cystic fibrosis; CFTR, cystic fibrosis transmembrane regulator; DIDS, 4,4' – diisothiocyanato-stilbene-2,2'-disulfonic acid; ENaC, epithelial Na⁺ channel; IGF-1, insulin-like growth factor; Isc, short circuit current, I-V, current-voltage: PGF2α, prostaglandin F2α; PKC, protein kinase C; PMA, phorbol 12myristate 13-acetate; UTP, uridine 5'-triphosphate

ACKNOWLEDGEMENT

The authors wish to thank So Yeong Lee for her invaluable comments on the manuscript.

REFERENCES

Awayda, M.S., I.I. Ismailov, B.K. Berdiev, C.M. Fuller, and D.J. Benos. 1996. Protein kinase regulation of a cloned epithelial Na⁺ channel. *J. Gen Physiol.* 108:49-65.

Awayda, M.S. 2000. Specific and nonspecific effects of protein kinase C on the epithelial Na⁻ channel. J. Gen. Physiol. 115:559-570.

Berdiev, B.K., R. Latorre, D.J. Benos, and I.I. Ismailov. 2001. Actin modifies Ca2+ block of epithelial Na+ channels in planar lipid bilayers. *Biophys. J.* 80:2176-2186.

Bourke, J., K. Abel, G. Huxham, V. Cooper, and S. Manley. 1999. UTP-preferring P₂ receptor mediates inhibition of sodium transport in porcine thyroid epithelial cells. *Br. J. Pharmacol*. 127:1787-1792.

Chan, H.C., C.Q. Liu, S.K. Fong, S.H. Law, L.J. Wu, E. So, Y.W. Chung, W.H. Ko, and P.Y. Wong. 1997. Regulation of Cl secretion by extracellular ATP in cultured mouse endometrial epithelium. *J. Membr. Biol.* 156: 45-52.

Chan, L.N., X.F. Wang, L.L. Tsang, and H.C. Chan. 2000. Pyrimidinoceptors-mediated activation of Ca²⁺-dependent Cl⁻ conductance in mouse endometrial epithelial cells. *Biochim. Biophys. Acta.* 1497:261-270.

Deachapunya, C., M. Palmer-Densmore, and S.M. O'Grady. 1999. Insulin stimulates transepithelial sodium transport by activation of a protein phosphatase that increases Na-K ATPase activity in endometrial epithelial cells. *J. Gen. Physiol.* 114:561-574.

Deachapunya, C., and S.M. O'Grady. 1998. Regulation of chloride secretion across porcine endometrial epithelial cells by prostaglandin E₂. J. Physiol. 508:31-47.

Deachapunya, C., and S.M. O'Grady. 2001. Epidermal growth factor regulates the transition from basal sodium absorption to anion secretion in cultured endometrial epithelial cells. *J. Cell. Physiol.* 186:243-250.

Devor, D.C. and J.M. Pilewski. 1999. UTP inhibits Na⁺ absorption in wild-type and ΔF508 CFTR-expressing human bronchial epithelia. Am. J. Physiol. Cell Physiol. 276:C827-C837.

Garty, H., and L.G. Palmer. 1997. Epithelial sodium channels: function, structure, and regulation. *Physiol. Rev.* 77:359-396.

Inglis, S.K., A. Collett, H.L. McAlroy, S.M. Wilson, and R.E. Olver. 1999. Effect of luminal nucleotides on Cl- secretion and Na+ absorption in distal bronchi. *Pflügers Arch.* 438:621-627.

Ishikawa, T., Y. Marunaka, and D. Rotin. 1998. Electrophysiological characterization of the rat epithelial Na⁺ channel (rENaC) expressed in MDCK cells; effects of Na⁺ and Ca²⁺. *J. Gen. Physiol.* 111:825-846.

Ismailov, I.I., B.K. Berdiev, V.G. Shlyonsky, and D.J. Benos. 1997. Mechanosensitivity of an epithelial Na⁻ channel in planar lipid bilayers: release from Ca²⁺ block. *Biophys. J.* 72:1182-1192.

Knowles, M.R., K.N. Olivier, K.W. Hohneker, J. Robinson, W.D. Bennett, and R.C. Boucher. 1995. Pharmacologic treatment of abnormal ion transport in the airway epithelium in cystic fibrosis. *Chest.* 107:71S-76S.

Kokko, K.E., P.S. Matsumoto, B.N. Ling, and D.C. Eaton. 1994. Effects of prostaglandin E₂ on amiloride-blockable Na⁺ channels in a distal nephron cell line (A6). Am. J. Physiol. Cell Physiol. 267:C1414-C1425.

Koster, H.P., A. Hartog, C.H. van Os, and R.J. Bindels. 1996. Inhibition of Na⁺ and Ca²⁺ reabsorption by P2U purinoceptors requires PKC but not Ca²⁺ signaling. *Am. J. Physiol. Renal Physiol.* 270:F53-F60.

Ling, B.N., K.E. Kokko, and D.C. Eaton. 1992. Inhibition of apical Na⁺ channels in rabbit cortical collecting tubules by basolateral prostaglandin E₂ is modulated by protein kinase C. J. Clin. Invest. 90:1328-1334.

- Mall, M., A. Wissner, T. Gonska, D. Calenborn, J. Kuehr, M. Brandis, and K. Kunzelmann. 2000. Inhibition of amiloride-sensitive epithelial Na⁺ absorption by extracellular nucleotides in human normal and cystic fibrosis airways. *Am. J. Respir. Cell. Mol. Biol.* 23:755-761.
- Mason, S.J., A.M. Paradiso, and R.C. Boucher. 1991. Regulation of transepithelial ion_transport and intracellular calcium by extracellular ATP in human normal and cystic fibrosis airway epithelium. *Br. J. Pharmacol.* 103:1649-1656.
- McCoy, D.E., A.L. Taylor, B.A. Kudlow, K. Karlson, M.J. Slattery, L.M. Schwiebert, E.M. Schwiebert, and B.A. Stanton. 1999. Nucleotides regulate NaCl transport in mIMCD-K2 cells via P2X and P2Y purinergic receptors. *Am. J. Physiol. Renal Physiol.* 277:F552-F559.
- Palmer-Densmore, M.L., C. Deachapunya, and S.M. O'Grady. 2000. Purinergic receptor mediated regulation of anion secretion in endometrial epithelial cells: Effects of adenosine and UTP. FASEB J. 14:595 (Abstr.)
- Ramminger, S.J., A. Collett, D.L. Baines, H. Murphie, H.L. McAlroy, R.E. Olver, S.K. Inglis, and S.M. Wilson. 1999. P2Y₂ receptor-mediated inhibition of ion transport in distal lung epithelial cells. *Br. J. Pharmacol.* 128:293-300.
- Shimkets, R.A., R. Lifton, and C.M. Canessa. 1998. In vivo phosphorylation of the epithelial sodium channel. *Proc. Natl. Acad. Sci. USA*. 95:3301-3305
- Stockand, J.D., H.-F. Bao, J. Schenck, B. Malik, P. Middleton, L.E. Schlanger, and D.C. Eaton. 2000. Differential effects of protein kinase C on the levels of epithelial Na⁺ channel subunit proteins. *J. Biol. Chem.* 275:25760-25765.
- Thomas, J., P. Deetjen, W.H. Ko, C. Jacobi, and J. Leipziger. 2001. P2Y₂ receptor-mediated inhibition of amiloride-sensitive short circuit current in M-1 mouse cortical collecting duct cells. *J. Membrane Biol.* 183:115-124.
- Vetter, A.E., C. Deachapunya, and S.M. O'Grady. 1997. Na absorption across endometrial epithelial cells is stimulated by cAMP-dependent activation of an inwardly rectifying K channel. J. Membr. Biol. 160:119-126.
- Wang, X.F., and H.C. Chan. 2000. Adenosine triphosphate induces inhibition of Na⁺ absorption in mouse endometrial epithelium: a Ca2+-dependent mechanism. *Biol. Reprod.* 63:1918-1924.

FIGURE LEGENDS

Figure 1. Effect of UTP on basal sodium transport. A: Representative trace showing that addition of 5 μ M benzamil to the apical solution blocked most of the basal Isc in monolayers maintained under serum free conditions, (n=9, N=4). B: Apical addition of UTP (1 μ M) caused a rapid increase in Isc followed by a slow decrease back to the basal Isc. Subsequent addition of benzamil had little inhibitory effect, but addition of NPPB (100 μ M at each arrow) blocked all of the remaining Isc, (n=15, N=4).

Figure 2. Effects of UTP and PMA on insulin-stimulated Na transport. A: Representative trace showing the time-dependent increase in Isc stimulated by 850 nM insulin added to the basolateral solution. Addition of 1 μ M UTP to the apical solution inhibited both the insulin-stimulated and basal Isc. **B:** Addition of 1 μ M phorbol 12-myristate 13-acetate (PMA) produced a similar decrease in insulin-stimulated and basal current as observed with UTP. **C:** Temporal changes in $[Ca^{2+}]_1$ in response to PMA and UTP were determined using fura 2-AM as described in the methods. Transient, elevations in $[Ca^{2+}]_1$ was observed following 1 and 5 μ M UTP in Ca^{2+} containing HBSS. No elevation in $[Ca^{2+}]_1$ was detected following 1 μ M PMA. (mean Ca^{2+} signal from 20 cells).

Figure 3. Current-voltage (I-V) relationships for the benzamil-sensitive pathway in the apical membrane. A: Experiments were performed using monolayers cultured in serum-free media with insulin for 3 days. Benzamil-sensitive difference currents were obtained using a voltage step protocol that ranged from -100 to +95 mV using 15 mV increments from a holding potential of 0 mV. Benzamil (5 μ M) was added apically to either permeabilized control cell monolayers (upper trace) or to permeabilized monolayers activated with 5 μ M UTP (lower trace). B: Benzamil-sensitive current-voltage relationships were obtained from amphotericin B-permeabilized monolayers in response to a voltage protocol that stepped from -90 to +90 mV in 15 mV increments from a holding potential of 0 mV. Benzamil (5 μ M) was added to the apical solution of permeabilized monolayers in the absence or presence of UTP (1 μ M).

Figure 4. Effect of UTP on Isc in the presence or absence of chloride. A: Representative trace showing chloride dependence of the UTP (5 μ M) response. Monolayers were bathed in standard porcine saline solution or chloride-free solution, replacing chloride with methane sulfonate. The peak UTP-activated current was reduced under chloride-free conditions (n=6). B: Bar graph showing the benzamil (5 μ M) and NPPB (100 μ M) -sensitive currents in the absence or presence of chloride. The NPPB-sensitive current was reduced under chloride-free conditions, whereas the benzamil-sensitive current remained the same, (n=6 for each).

Figure 5. Effect of UTP on apical membrane Cl conductance. A: Representative trace showing the transient change in apical membrane current after stimulation with 1 μM UTP using monolayers where the basolateral membrane was permeabilized with amphotericin B (10 μM). The basolateral membrane was bathed with KMeSO₄ saline solution, while the apical membrane was bathed with standard porcine saline solution. B: Current-voltage relationship showing the UTP-activated current obtained in response to voltage steps from -90 to +90 mV in 15 mV increments from a holding potential of 0 mV.

Figure 6. PKC inhibitors prevent the inhibition of benzamil-sensitive Isc after UTP. A: Representative trace showing the benzamil-sensitive current in the absence or presence UTP (5 μ M), and after pretreatment with both Gö6983 (10 μ M) and UTP, (n=8, 14 and 9, respectively, N=3). B: Bar graph illustrating the benzamil-sensitive current after only benzamil (5 μ M, n=8), after UTP (5 μ M, n=14), after PMA (0.5 μ M, n=4), after UTP in the presence of Gö6983 (10 μ M, n=9), after UTP in the presence of rottlerin (2.5 μ M, n=5), or after UTP in the presence of Gö6976 (100 nM, n=6 and 10 μ M, n=4, respectively). C: The calculated benzamil-sensitive, apical membrane conductance at 0 mV, before and after the addition of UTP (5 μ M) and after pretreatment with both GF109203X (5 μ M) and UTP, (n=3).

Figure 7. Western blot analysis of PKC isoforms in monolayers maintained under serum free conditions. Antibodies used for these western blots were generated using human PKC isoforms in rabbit as indicated in the methods. Antibody labeling observed in whole cell lysates were from epithelial cells maintained under serum-free conditions for 76 hours.

Figure 8. Effect of BAPTA-AM on changes in $[Ca^{2+}]_i$ in response to UTP. A: Temporal changes in $[Ca^{2+}]_i$ in response to UTP were determined using fura 2-AM as described in the methods. Upon stimulation with 5 μ M UTP in Ca^{2+} -containing HBSS, control cells initially produced a transient elevation in $[Ca^{2+}]_i$, followed by a gradual decline to a new sustained elevated $[Ca^{2+}]_i$. Removing UTP from the bathing solution returned the intracellular calcium concentrations back to baseline levels. B: BAPTA-AM reduced the basal level of intracellular calcium by 80 nM, and upon stimulation with UTP, $[Ca^{2+}]_i$ increased by only 20 nM. For this figure, measurements were obtained from 20 cells in each of three separate experiments.

Figure 9. BAPTA-AM does not effect the UTP-mediated inhibition of sodium absorption.

A: Representative trace showing that the peak UTP-activated Isc response is diminished after pretreatment with 50 μM BAPTA-AM. **B:** Representative trace showing that UTP (5 μM) reduced the benzamil-sensitive current, even in the presence of BAPTA-AM. **C:** Bar graph illustrating that pretreatment with BAPTA-AM diminished the UTP-activated current, but failed to affect inhibition of the benzamil-sensitive current by UTP, (n=6 for each).

Figure 10. Model. Transepithelial Na absorption is inhibited following stimulation with UTP. UTP activates multiple PKC isoforms that in turn inhibit epithelial Na channels present in the apical membrane. (See text for further details.)

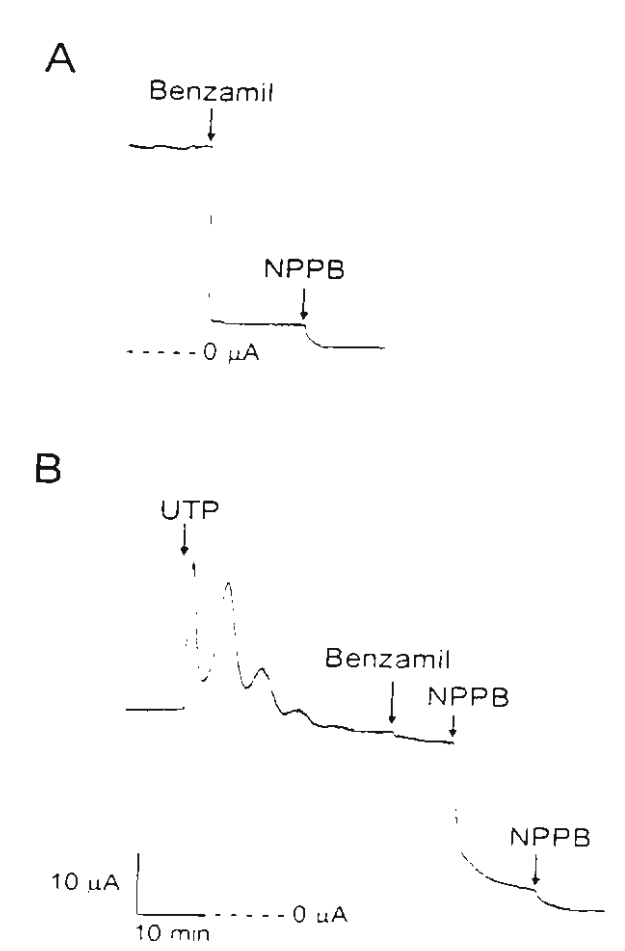
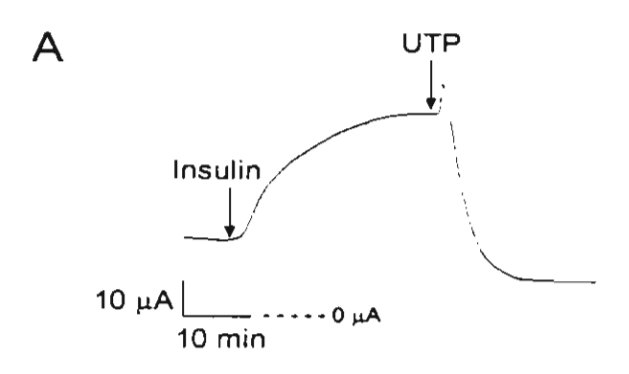
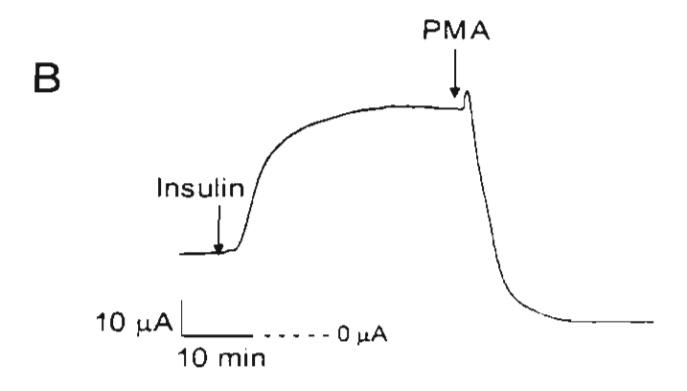


Figure 1





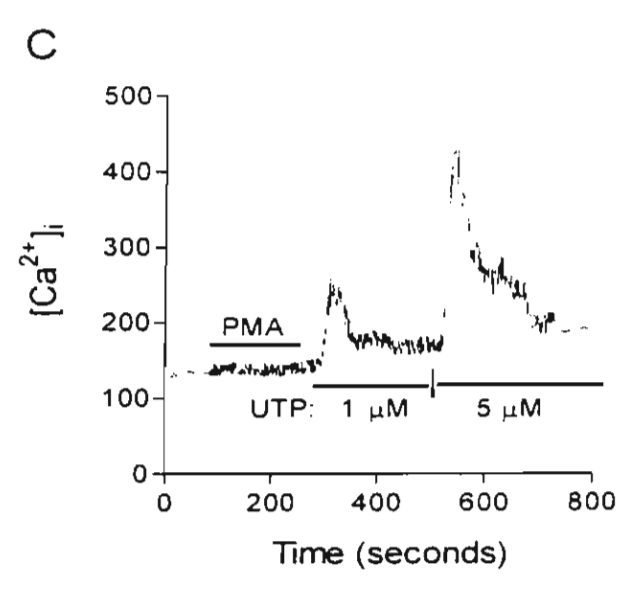


Figure 2

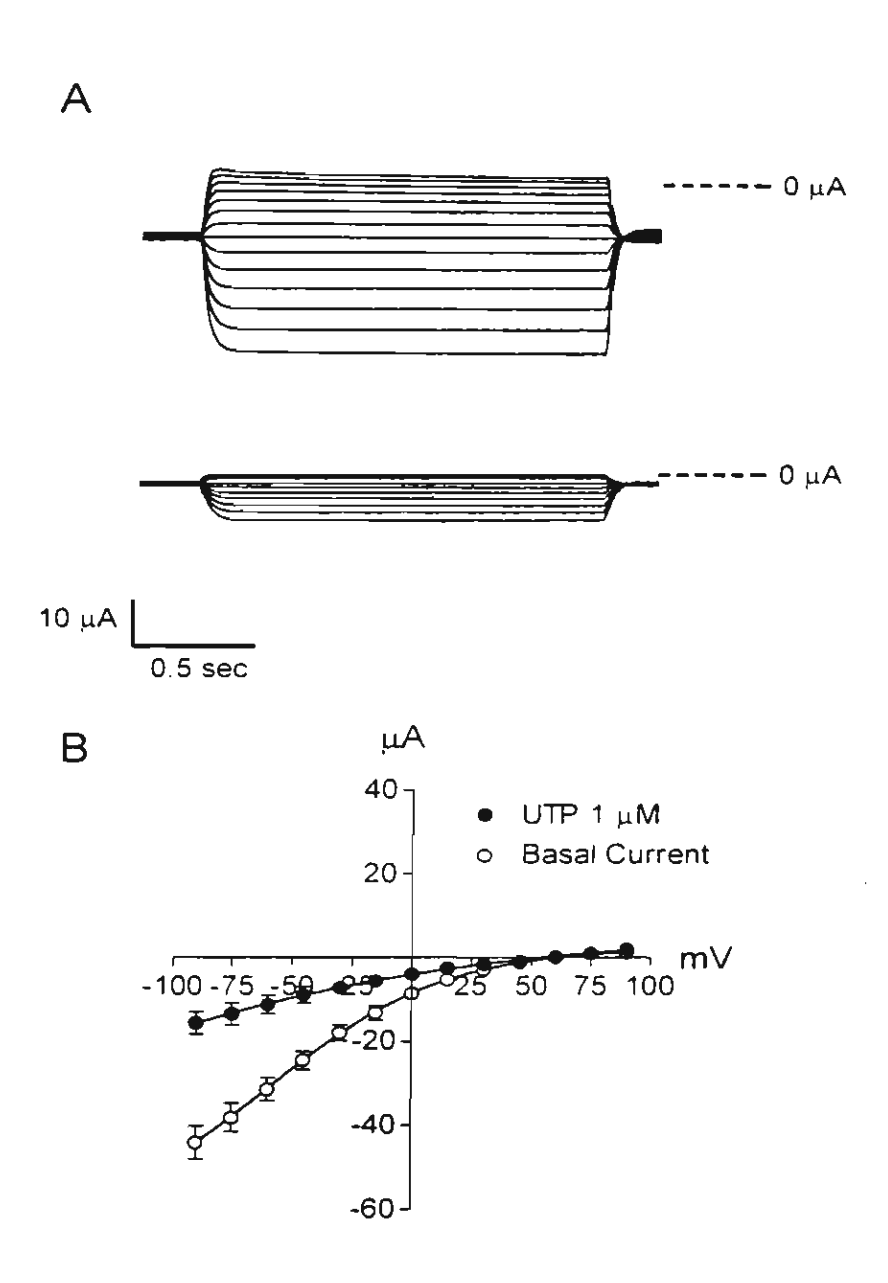
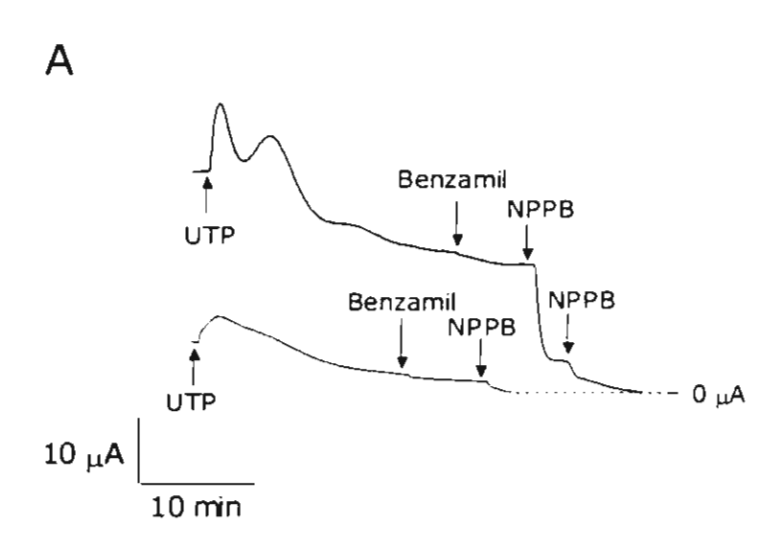


Figure 3



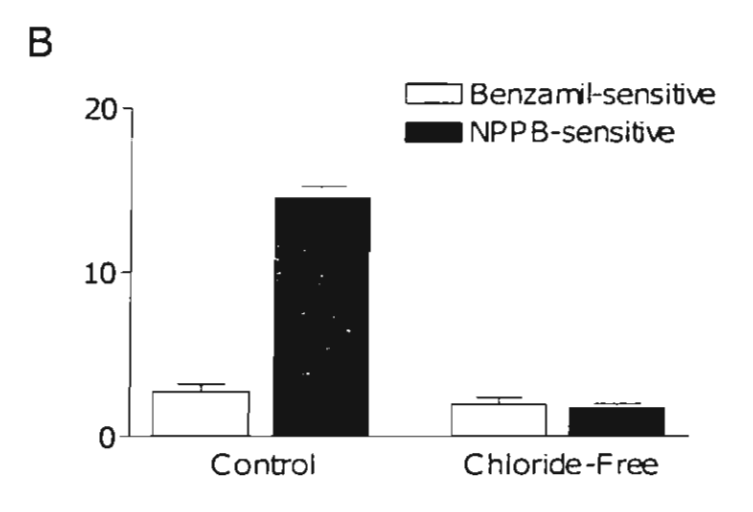
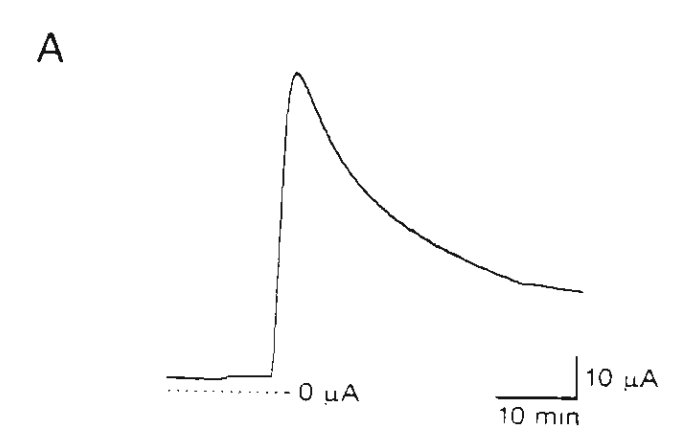


Figure 4



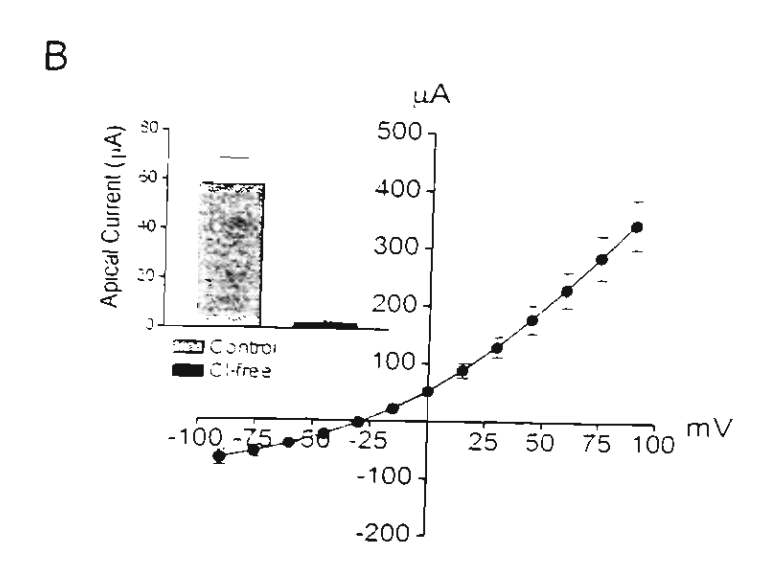


Figure 5

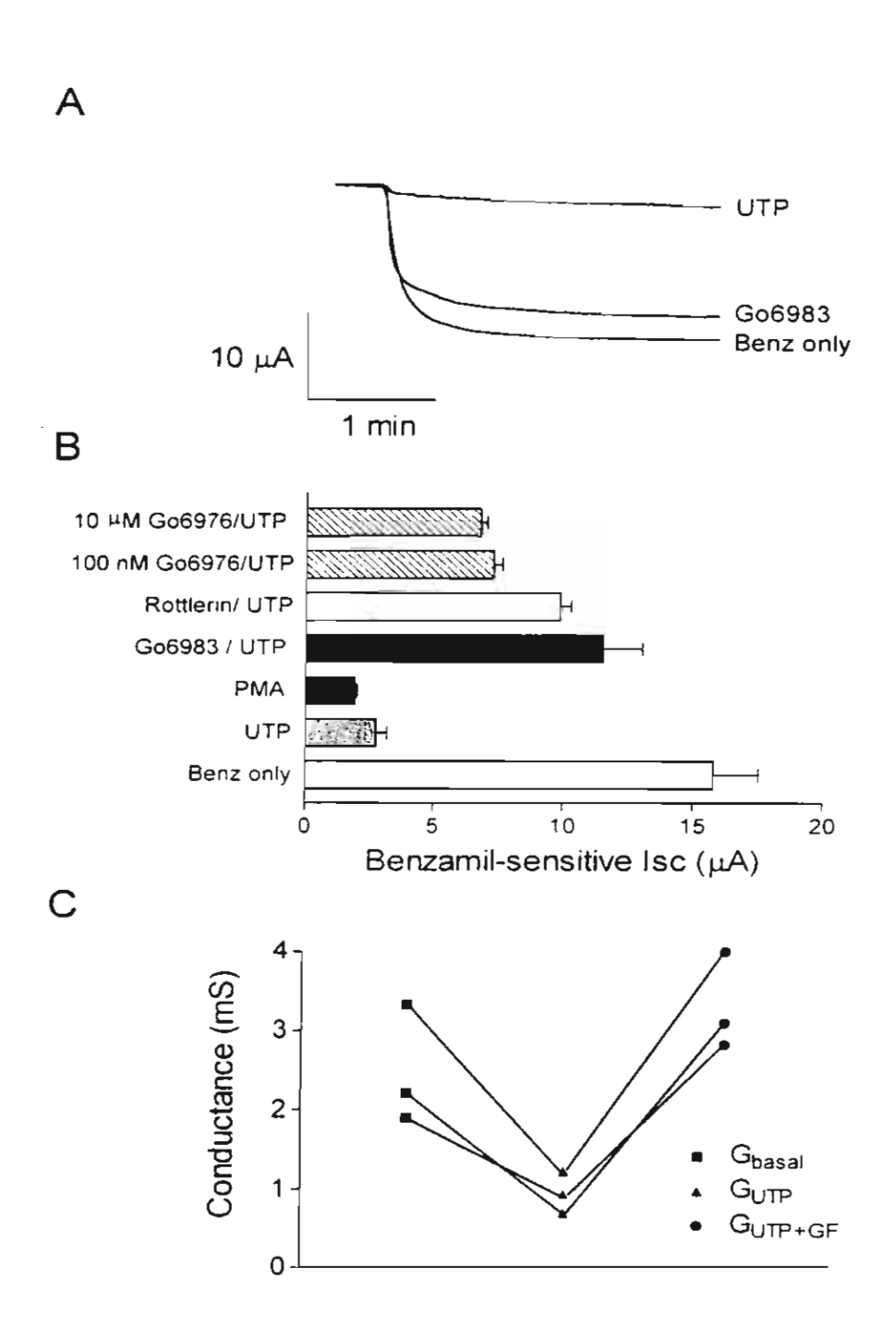


Figure 6





45 7 kD —

32.5 kD ----

Figure 7

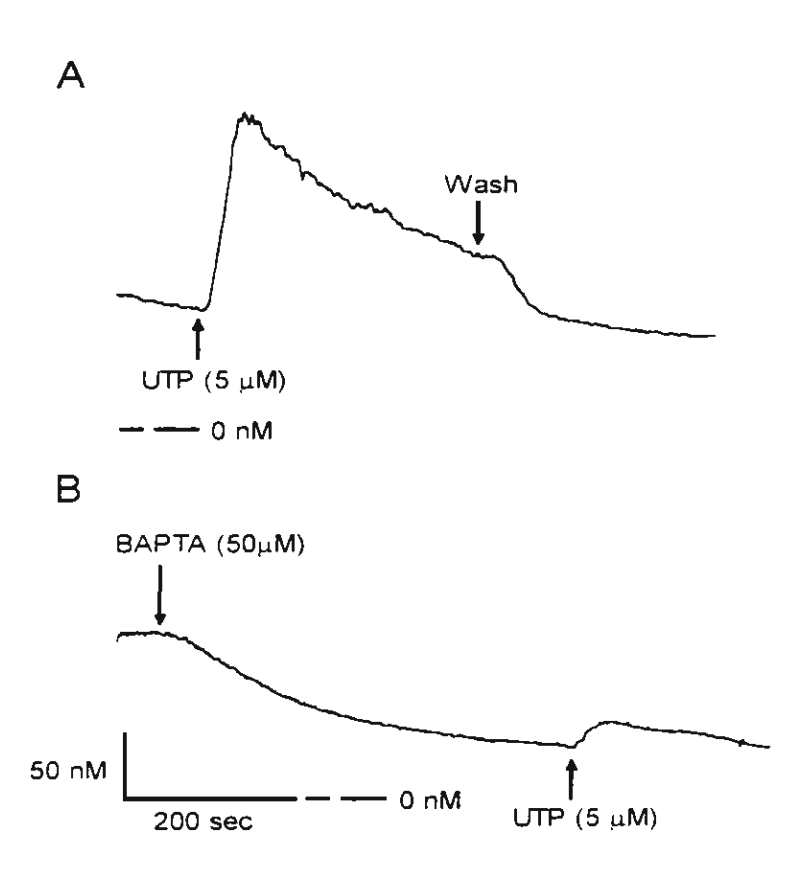


Figure 8

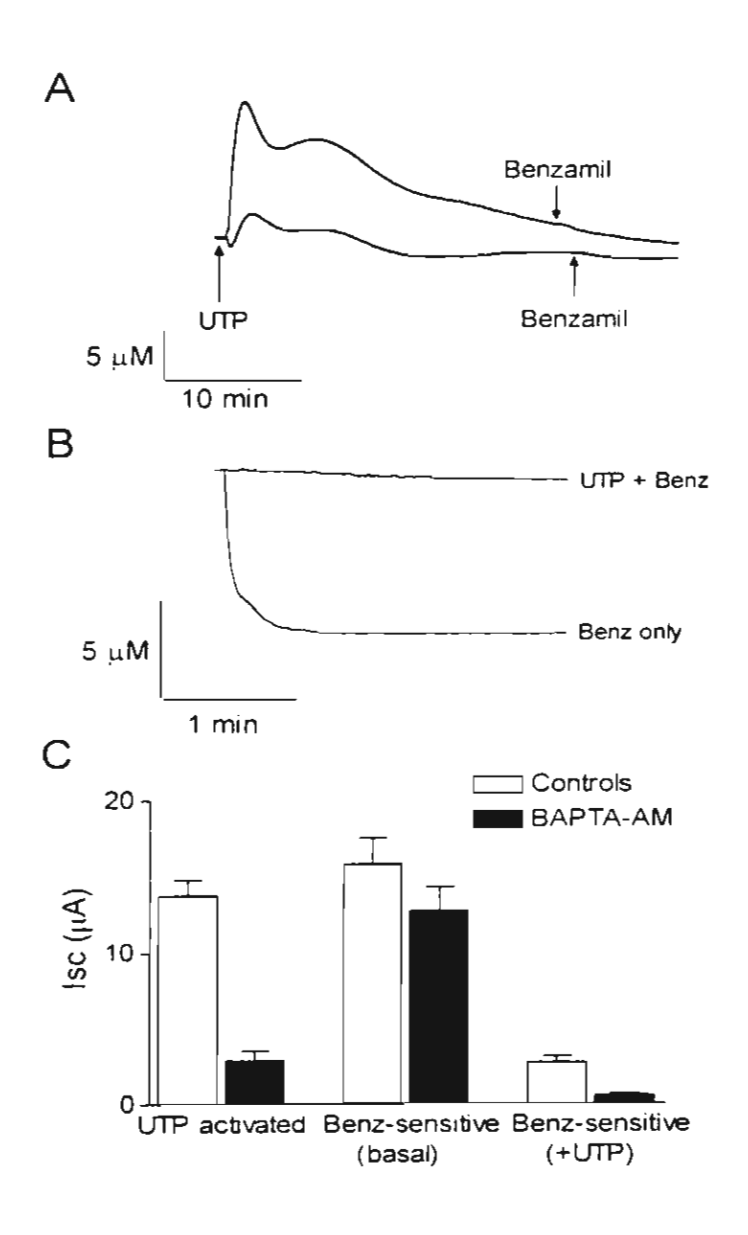


Figure 9

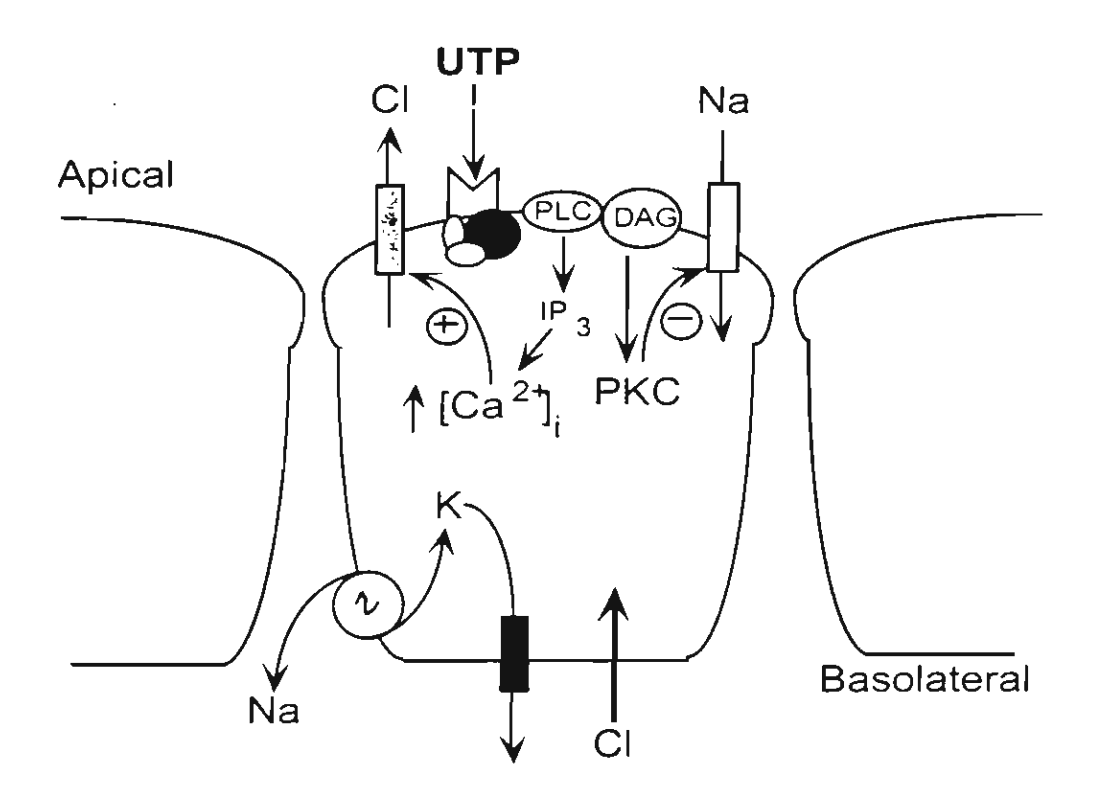


Figure 10